



Bulletin 2

Second periodic report

1 Publishable summary

The largest uncertainty in current estimates of the planetary radiation budget is due to atmospheric aerosols and has caused the International Panel on Climate Change (IPCC) to call for an urgent expansion of global studies to help monitor and characterise aerosols. Aerosol properties are most routinely monitored by the ground-based aerosol robotic network (AERONET). However, while there is a high density of AERONET instruments in populated areas and megacities, the most dominant sources of aerosol originate from often uninhabited regions like the planet's deserts, oceans and ice-caps where few instruments exist. There is therefore a lack of knowledge of the overall global spatial and temporal variation of aerosols. The AEROMAP project was designed to provide a solution to overcome this lack of information without the need to invest in hundreds of new AERONET sites. To achieve this, AEROMAP is capitalizing on the full-Earth measurements provided daily by satellite remote sensing instruments to produce the first global maps of the aerosol microphysics like the distribution of particle sizes. Furthermore, AEROMAP is opening a window on aerosol characteristics over the oceans and deserts which are of paramount importance to the estimate of the overall Earth radiation budget.

AEROMAP has developed and validated new data mining tools based on cluster analysis and neural networks to convert satellite measurements into aerosol optical and microphysical properties for different globally-distributed aerosol types. Retrieval of parameters like the aerosol size distribution, refractive index, single scattering albedo and asymmetry factor have, until now, not been possible from space. The inputs to AEROMAP's inversion algorithm are a small but specific set of satellite measurements. Specifically, daily, full-Earth measurements of the aerosol optical depth (AOD) at 470, 550 and 660nm and the columnar water vapour provided by the moderate resolution imaging spectrometer (MODIS) onboard the twin polar satellites Terra and Aqua, in conjunction with the absorption AOD at 500nm provided by the ozone monitoring instrument (OMI) onboard the Aura satellite. The outputs from AEROMAP are direct and instantaneous retrievals of 45 microphysical and optical parameters needed to characterise aerosols. This is accomplished by optimizing and training neural networks to learn the relation between satellite inputs and co-located and synchronous AERONET outputs. Since best results are obtained by training a different neural network for each distinct aerosol source region, cluster analysis has been applied to 7 years of daily-averaged data from the NASA/GEOS-5 mission's global ozone chemistry aerosol radiation and transport (GOCART) model to create geographical partitioning using 10 distinct aerosol types/mixtures. Satellite data in each pixel of size $1^\circ \times 1^\circ$ (latitude x longitude) spanning the globe is then fed to the corresponding neural network for that pixel to generate aerosol optical and microphysical parameters. The daily global maps produced allow for monitoring and classification of aerosols as they move across the Earth's surface.

The main objectives of AEROMAP during this reporting period were to use cluster analysis to partition the globe by aerosol type/mixture, and to then code neural networks to learn the relation between daily-averaged satellite inputs and aerosol microphysical parameters as outputs for each different aerosol type/mixture. A further objective was to generate daily or near-daily global maps of such parameters and to track the temporal evolution of important events such as desert dust storms, forest fire outbreaks, urban brown cloud pollution episodes, and volcanic eruptions. Another goal, related to this, was for AEROMAP to test the feasibility of creating a global near real-time monitor of aerosols and an alerting service based on the construction of an air quality index for the assessment of climatological risks and the issuing of early-warnings. A final objective during this period was to disseminate the results of the project widely so as to showcase it as an important product from the European Research Area to attract future collaboration. The global maps of aerosol microphysical parameters being produced by AEROMAP, it is hoped, will assist in the construction of new infrastructures in relation to aerosol-related hazards.

The AEROMAP project is unique in many ways. Firstly, it helps address the need for global monitoring and characterization of aerosols by producing the first global maps of aerosol parameters that were not available from space. Secondly, AEROMAP provides detailed microphysics of aerosol originating from dominant natural sources of aerosols over the oceans, deserts and ice caps for the first time. Thirdly, the classification of aerosol types/mixtures produced by AEROMAP's cluster analysis algorithm provides a geographical partitioning of global aerosol source regions into distinct compositional mixtures that will be of value to future studies and help decision-makers understand where best to place new ground-based

remote sensing instruments for detailed local studies. Fourthly, AEROMAP has produced the first global maps of air quality index using aerosol microphysics rather than chemistry. Finally, AEROMAP has innovated highly in the fields of aerosol science, environmental research and atmospheric physics by applying contemporary methods of machine learning, mathematical data analysis, and statistics to substantially increase our understanding of the global Earth-aerosol system.

The project has brought together the skills of the fellow Dr Michael Taylor as an experienced researcher in the fields of applied mathematics and computational physics, with the expertise of the scientist in charge (SIC) Dr Stelios Kazadzis in the fields of atmospheric physics, satellite remote sensing, ground-based measurement and retrieval of aerosol properties at the National Observatory of Athens - a world leading centre for aerosol monitoring. The highly multidisciplinary nature of AEROMAP has meant that it has been able to successfully capitalize on the synthesis and exchange of knowledge between the fellow and the SIC, leading to 4 peer-reviewed publications in top journals in the fields of atmospheric physics and chemistry, atmospheric measurement techniques, as well as 2 conference papers submitted for publication in the proceedings of the prestigious 12th International Conference on Meteorology, Climatology and Atmospheric Physics to be held in Heraklion, Crete in May. In this, the network of contacts of the SIC was instrumental in establishing new collaborations for the fellow in the field of environmental research. As of the 28th of February 2014, the 4 peer-reviewed research articles published have already accrued a total of 937 HTML online views and 658 PDF downloads. It is hoped that the large number of research articles produced by AEROMAP will engage a large audience about the project's contribution to the global characterization of aerosols.

1.2 Description of the work performed and the main results achieved so far

During the first 12 months of the project (please refer to Sections 2 and 3 of the mid-term report for details):

- satellite inputs comprising over eight years of daily measurements (2004-2013) of the AOD at 470, 550, 660nm and the columnar H₂O from the MODIS Aqua Level 3 Collection 5.1 together with the absorption AOD at 500nm from the Ozone Measuring Instrument (OMI) Level 3 OMAERUV algorithm were derived at a spatial resolution of 1×1 degree (latitude x longitude). In conjunction with this, co-located (in the same pixel) and synchronous daily-averaged ground-based AERONET Level 2.0 Version 2 Inversions Product parameters spanning the years 1993-2013 and including the AVSD retrieved in 22 logarithmically-equidistant radial bins spanning the range of particle radii from 0.05 to 15µm, the real and imaginary parts of the CRI(λ), the SSA(λ) and the asymmetry parameter ASYM(λ) centred at λ = 440, 675, 870 and 1020nm were downloaded and pre-processed to filter for complete records (**Task: A1**),
- the functional relation between the AOD measured by satellite and ground-based remote sensors was found by linearly-regressing derived MODIS AODs on co-located and synchronous AERONET direct-sun AOD values and validated for AERONET sites having long data records (GSFC-Washington and MSUMO-Moscow). A poster to engage the public was presented at the European Science Open Forum 2012 in Dublin, Ireland (**Tasks: A2 & E3, Objective: 9, Deliverable: 3**),
- the functional relation between AERONET direct-sun AODs and AERONET Level 2.0 Version 2 inversion products (the AVSD, CRI, ASYM and SSA) was deduced by training and validating neural networks (NNs) with data from the following AERONET individual sites known to be dominated by dust, biomass burning and urban sulphate (SO₂) aerosol: Banizoumbou (Niger), Alta Floresta (Brazil) and GSFC-Washington (USA) respectively. AEROMAP developed a new methodology for optimizing neural network architectures and for identifying optimal network configurations. The ability of the optimal NN architecture in each case to extrapolate to another qualitatively-similar but distant site was tested by presenting them with unseen data at the following dust, biomass-burning and urban SO₂ sites: Solar Village (Saudi Arabia), Mongu (Zambia) and MSU-MO-Moscow respectively (**Task: A3, Objectives: 1 & 2, Deliverable: 1**),

- the functional relation between satellite-derived AOD and AERONET Level 2.0 Version 2 inversion products (the AVSD, CRI, ASYM and SSA), was deduced by training and validating a new NN with complete records of co-located and synchronous data at GSFC-Washington and then testing its ability to extrapolate to data in the pixel containing MSUMO-Washington. The results were presented at the European Aerosol Conference 2012 in Granada, Spain (**Tasks: A3 & E3, Objectives: 4 & 9, Deliverable: 2**),
- the ability of satellite-input NNs to extrapolate using capped data was investigated by training NNs with co-located and synchronous data from a cluster of pixels of similar aerosol composition (as per the chemical composition provided by the GOCART model) for the cases: dust, biomass burning and urban SO₂. In each case half of the data was used for NN training and validation and half was used for testing. The NNs were validated also at the weekly, monthly and seasonal timescales (**Task: B1**),
- the ability of satellite-input NNs to extrapolate to regions where no sites exist, was investigated by feeding the Northern Africa dust-trained NN with satellite inputs at the distant dust locations Solar Village (Arabian desert) and Dalanzadgad (Gobi desert), and the Amazonian biomass burning cluster-trained NN with satellite inputs at Mongu (Zambia) – all well outside the geographical domain of the datasets used to train, validate and test the NNs in (5): (**Task: B2, Objective: 4**),
- the project website was designed and created (<http://apcg.space.noa.gr/aeromap>) to help inform the general public and the environmental research community about the project and its scope. In addition, educational resources were uploaded on the website as a gateway to engage the public about the important role of aerosols on climate change and the contribution of the project to this issue (**Tasks: E1 & E4, Objective: 9, Deliverable: 9**),
- a peer-reviewed assessment report on the function approximation ability and extrapolation power of NNs trained with MODIS data (AOD at 470, 550 and 660nm and water vapour) and OMI data (absorption AOD at 500nm) inputs and AERONET outputs for the case of desert dust was submitted and published in an open access EGU journal: Taylor, M., Kazadzis, S., Tsekeri, A., Gkikas, A., Amiridis, V. (2013) Satellite retrieval of aerosol microphysical and optical parameters using neural networks: a new methodology applied to the Sahara desert dust peak. *Atmospheric Measurement Techniques Discussions*, 6, 10955-11010 (**Milestone 1**),
- the mid-term report was deposited at the ESS on the 19th of April 2013 (**Milestone 2**).

1.2.1 Results for the second reporting period

During the second 12 months of the project (please refer to Sections 2 and 3 of this report for details):

- the complete global data record of 3-hourly measurements of AOD per aerosol type at 1×1 degree (latitude x longitude) spanning the years 2000-2006 (inclusive) from the global ozone chemistry aerosol radiation and transport (GOCART) model was downloaded and converted into daily-averages. Cluster analysis was then performed on the mean global values and used to partition the global 1x1 degree grid into 10 distinct aerosol type/mixture regions (**Task: C1, Objective 5: Deliverable 5**),
- the temporal variation of NN-derived AMPs in the dust cluster was monitored at the monthly, weekly and daily timescale and validated (**Task: C2, Objective: 6, Deliverable 7**)
- two pilot studies were performed: 1) to help calibrate Saharan dust LIDAR AOD retrievals for CALIPSO and 2) to compare AERONET-retrieved microphysical parameters obtained at Athens with higher temporal frequency values provided by the precision filter radiometer instrument (**Task: C2, Objective: 6: Deliverable: 7**),
- global NN-derived AMP maps were rendered using the aerosol typing provided by the cluster analysis of Task C1 (**Task: C3, Objective: 7, Deliverable 6**).
- high accuracy daily global NN-derived AMP maps were rendered at 1x1 degree spatial resolution (**Task: C3, Objective: 7, Deliverable 8**).

- the feasibility of performing near-realtime monitoring was then assessed by modelling the spatio-temporal evolution of sulphate emission from the Karthala volcanic eruption in Madagascar (**Task: D1, Objective: 8, Deliverable: 9**)
- two air quality indices to measure the impact of aerosol on health and visibility were constructed and mapped globally at 1x1 spatial resolution. In addition, the indices were normalized to a the European standard categorical scale and alert advice was produced for each category (**Task: D2, Objective: 8, Deliverable: 9**)
- a large volume of new content was added to the project website to raise public awareness about the project, its aims and expected results, and the role of Marie-Curie Actions in supporting research in the ERA aerosols (**Task E2: Objective: 9, Deliverable 10**)
- large-scale dissemination of results was accomplished via publication of 6 peer-reviewed research articles (**Task: E3, Objective: 9, Deliverable 10**)
- a public talk on the role of aerosols, their impact on climate change and the way AEROMAP's global outputs contribute to advancing our understanding of their global distribution and characterization (**Task: E4: Objective: 9, Deliverable 10**)
- the second periodic report was deposited at the ESS (**Milestone 3**)
- the final report was deposited at the ESS (**Milestone 4**)

In addition to results following from implementation of the proposed Work Plan, a number of additional (unforeseen) bi-products were also produced. In particular,

- a new technique was developed for improving the fit to the retrieved aerosol size distribution, based on Gaussian mixture models which allows for automatic identification of the number of distinct aerosol modes present. This technique was also applied to monitor the temporal evolution of high load aerosol events and atypical events (**Publications 2,6 and 7 – see list below**),
- a new technique for optimising the retrieval of Saharan dust parameters from LIDAR measurements with CALIPSO was developed and validated (**Publication 3**),
- a comparison of AERONET-retrieved microphysical parameters obtained at Athens during with higher frequency parameters produced by the World Meteorological Organisation's precision filter radiometer was performed (**Publication 4**),
- two air quality indices for the impact of aerosol on health and visibility were constructed and mapped globally at 1x1 spatial resolution

In this reporting period great emphasis was made on dissemination of results. AEROMAP produced the following peer-reviewed publications (including papers under peer-review or at submission stage):

- Taylor, M., Kazadzis, S., Tsekeri, A., Gkikas, A., Amiridis, V. (2013). Satellite retrieval of aerosol microphysical and optical parameters using neural networks: a new methodology applied to the Sahara desert dust peak. *Atmospheric Measurement Techniques Discussions* 6, 10955-11010, 2013.
- Taylor, M., Kazadzis, S., Gerosopoulos, E. (2013). Multi-modal analysis of aerosol robotic network size distributions for remote sensing applications: dominant aerosol type cases. *Atmospheric Measurement Techniques Discussions* 6, 10571–10615, 2013 (accepted and in press at AMT)
- Amiridis, V., Wandinger, U., Marinou, E., Giannakaki, E., Tsekeri, A., Basart, S., Kazadzis, S., Gkikas, A., Taylor, M., Baldasano, J., & Ansmann, A. (2013). Optimizing Saharan dust CALIPSO retrievals. *Atmospheric Chemistry and Physics* 13, 12089-12106.
- Kazadzis, S., Veselovskii, I., Amiridis, V., Gröbner, J., Suvorina, A., Nyeki, S., Gerasopoulos, E., Kouremeti, N., Taylor, M., Tsekeri, A., Wehrli, C. (2014). Aerosol microphysical retrievals from Precision Filter Radiometer direct solar radiation measurements and comparison with AERONET. *Atmospheric Measurement Techniques Discussions* 7, 99-130, 2014.

5. Taylor, M., Kazadzis, S., Tsekeri, A., Gkikas, A., Amiridis, V. (2014). AEROMAP: Satellite retrieval of dust aerosol microphysical and optical parameters using neural networks. *Proc. 12th Int. Conf. on Meterology, Climatology and Atmos. Phys. (COMECA), 28-31/05/2014, Heraklion, Crete, Greece.* (under review).
6. Taylor, M., Kazadzis, S., Gerosopoulos, E. (2014). Multi-modal fitting of AERONET size distributions during atypical aerosol conditions. *Proc. 12th Int. Conf. on Meterology, Climatology and Atmos. Phys. (COMECA), 28-31/05/2014, Heraklion, Crete, Greece.* (under review).
7. Taylor, M., Kazadzis, S., Gerosopoulos, E. (2014). Multi-modal analysis of aerosol robotic network size distributions for remote sensing applications II: temporal evolution of high load events. *Atmospheric Chemistry and Physics Discussions* (manuscript ready for submission).

1.2.2 Socio-economic impact of AEROMAP's results and the wider societal implications

1.2.2.1 Contribution to European excellence and European competitiveness

AEROMAP is actively contributing to the provision of new information on one of the most important climate change parameters - the global distribution and characterization of aerosols. The interest that the published results of the project are generating as indicated by the large number of downloads and online views, it is hoped, will significantly help to raise the profile of the host institute as a centre of excellence in the field and therefore the European Research Area (ERA) for researchers. This, combined with the growing volume of click-throughs on the project website are an early indication that the end-products of this project will continue to contribute to European excellence and competitiveness by demonstrating that European centres like the host institute NOA are pioneering new mathematical/computational methods in aerosol science and remote sensing. The fellow, the host institute and hence Europe as originator of such methodologies are likely to act as a pole of attraction to scientists from outside the ERA who are interested in learning such techniques and applying them to their own fields of research. Furthermore, the near-realtime monitor and the aerosol impact index and alerts developed, together with other important products such as unique high spatial resolution global maps of aerosol microphysical properties being produced, will help foster collaborations and the writing of new research proposals building this new source of knowledge. The showcasing of the project at the website/portal, the large effort invested in rapidly publishing research results and techniques in several top journals in field, as well as presentation of interesting findings at 3 international conferences have helped to strongly advertise AEROMAP, the fellow, the host institute NOA and the Marie Curie Actions. We hope that the potential impact of AEROMAP on global environmental policy-making decisions will have positive repercussions that will further turn eyes towards the ERA.

1.2.2.2 How AEROMAP will produce long-term synergies and/or structuring effects

Until now, it has not been possible to exploit the full-Earth coverage provided by satellite remote sensing in order to globally-characterise aerosols via their microphysical properties. As a result, Europe has followed the example of other continents in installing expensive ground-based remote sensing instruments federated to AERONET. While the methodology proposed here to extrapolate from local AERONET sites to non-existent site locations yield accurate deductions of aerosol microphysical properties and aerosol mixtures (via cluster analysis), there is no doubt that the best way to validate neural network-derived retrievals, is with co-located AERONET data. One direct long-term structuring effect of AEROMAP is that its products will help funding agencies at the national or regional level better determine where to best locate new aerosol monitoring stations. Small scale but high impact projects like AEROMAP will help to ensure that Europe can meet the challenges of the 21st century where the quality of the environment affects everyday life and the impact of aerosols on climate change, air quality and business (e.g. aviation) is high in the public conscience. AEROMAP represents a concerted effort to bring satellite remote sensing and ground-based data-providers and scientists together to maximise their utility and impact and, as a result, the project is an important showpiece for European science and fellowships and actions like the Marie Curie IEF.

Considering the cost of satellite data acquisition, and especially the large data quantities involved with global modelling, AEROMAP has placed great emphasis on efficient data exploitation. A priority has been on the development and dissemination of general techniques that can potentially be incorporated in existing operational algorithms. For example, the multi-modal method developed to improve fits to the size distribution has stimulated discussions about how our technique can possibly be incorporated as a post-processing module to existing operational inversion algorithms.

Scientists can now collect maps of large-scale (1x1 degree) aerosol episodes on the timescale of days to weeks and can create AVI movies (1 frame per day) to trace their dispersal. Our analysis of climatologically and/or socio-economically important strong aerosol events including dust storms, forest fire outbreaks, urban brown clouds and volcanic eruptions will also help add further value to the products and results produced by AEROMAP. The project has demonstrated its ability to monitor and characterise global aerosols and their temporal variation to the aerosol science community and the new global maps of air quality indices have the potential to impact local authorities' decision-making capabilities and the taking of evasive action during intense aerosol exposure episodes.

1.2.2.3 Impact of outreach activities

During the first 12 months of the project, the fellow participated in the European Open Science Forum 2012 in Dublin, Ireland with a digital poster presentation of the planned methodology to be implemented by AEROMAP and the importance of global monitoring of aerosols. He presented a technical poster session on initial results from Tasks A1-A3 at the European Aerosol Conference 2012 in Granada, Spain. His work was displayed as part of the activities of the Atmospheric Physics and Chemistry (ACP) Group at the National Observatory of Athens (NOA) at the FP7-funded Researcher's Night 2012 at the National Hellenic Research Foundation. He also gave two seminars reporting back on the progress of the project and the results emerging from Phases A and B. The fellow has an active profile page on the ACP Group website (<http://apcg.space.noa.gr>) where copies of his talks and conference posters are exhibited. In addition, the fellow created a Twitter account (handle: _AEROMAP) for tweeting updates and news about the project, and he designed a website/portal for the project (<http://apcg.space.noa.gr/AEROMAP>) that has prominent hyperlinks to the personal webpages of the fellow, the scientist in charge, and the host institute, and which describes the important role played by Marie-Curie actions in facilitating European research and mobility in an abstract describing the project, its objectives and a timeline for monitoring progress (please refer to Section 2.3.6 for details of the development of the project website).

During the second 12 months of the project, the fellow:

1. developed the Researchers' Gateway and Education Gateway areas of the project website to engage scientists and the non-technical reader (please refer to Section 2.3.6 for details),
2. participated in the CERN OA18 Workshop on Innovations in Scientific Communication to learn how researchers can use new web-based technologies to improve the dissemination of their results,
3. started using Twitter to find, follow and engage with interested readers in the fields of aerosol science, environmental research and science communication (https://twitter.com/_AEROMAP),
4. established international collaborations leading to co-authorship and publication of two articles in leading journals in the field,
5. engaged in the publication (as first author) of articles reporting the research results of AEROMAP,
6. submitted conference papers for publication in the proceedings of the *Prestigious International Conference on Meteorology, Climatology and Atmospheric Physics* (COMECP) to be hosted by Greece this May – further disseminating the results of the project post-completion.

At the end of the project, the fellow will write and issue a press release announcing in the national and academic press, and on social media, the completion of the project and its main findings. The outreach activities above, led by the fellow, have helped and will continue to help increase the national, European and international impact of AEROMAP.

1.1.3 Diagrams or photographs illustrating and promoting the work of the project

A detailed graphical abstract has been produced to help visualize the overall methodology implemented by AEROMAP and has been included in the host institute's research portfolio:

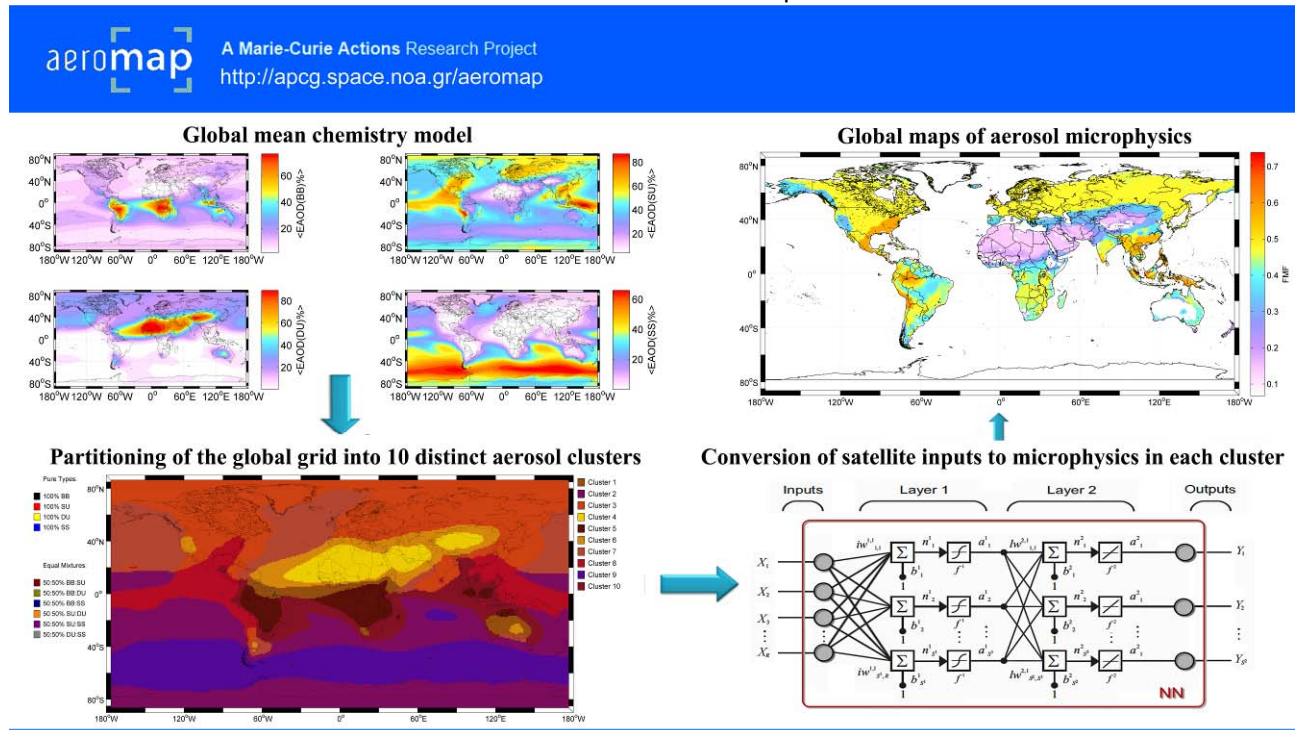


Figure 1: New graphical abstract illustrating the AEROMAP methodology

1.1.4 Contact details

Dr Stelios Kazadzis (**SIC**) APCG, IERSD-NOA

Dr Michael Taylor (**fellow**) APCG, IERSD-NOA (email: patternizer@gmail.com)

Atmospheric Physics and Chemistry Group (APCG: <http://apcg.space.noa.gr>),
Institute for Environmental Research and Sustainable Development (IERSD),
National Observatory of Athens (NOA: <http://www.noa.gr>),
I. Metaxa & Vas. Pavlou, Lofos Koufou, GR 152 36, P. Penteli, Athens, Greece.
Tel: +30 (0)210 8109151
Fax: +30 (0)210 8103236

2 Project objectives, work progress and achievements & project management

2.1 Project objectives for the period

The reporting period spans one year from 01/03/2013 to 28/02/2014 and includes the following stated phases of the project shown in the project timeline below:

- Phase C (months 9-15): Cluster analysis, aerosol typing and case studies:
C1 (months 9-12): Cluster analysis of global AERONET sites
C2 (months 9-15): Pilot studies
C3 (months 12-15): Production of global maps based on Gobbi coordinates
- Phase D (months 15-24): 3D spatio-temporal mapping and real-time monitoring/alerting
D1 (months 15-18): Initiation of the real-time monitor
D2 (months 18-24): Implementation of the real-time monitor and alerting service
- Phase E (Months 1-24): Website design, maintenance and public engagement:
E2 (month 12): Public engagement on the role of Marie-Curie Actions and on atmospheric chemistry
E3 (months 12-21): Outreach mass media activities
E4 (month 23): Public engagement on aerosol pollution and climate change

Timeline(months) /Phases	0-3	3-6	6-9	9-12	12-15	15-18	18-21	21-24
Phase A:		A1,A2	A2,A3					
Phase B:				B1,B2				
Phase C:					C1,C2	C2, C3		
Phase D:						D1	D2	D2
Phase E:	E1	E1	E1	E2	E3	E3	E3	E4
Milestones			M1	M2			M3	M4

The project objectives, relevant to the second 12 months of the project spanning Phases C1-3, D1-2 and E1-4 are as follows:

Objective 5: to classify and characterise the global ANN-derived AMP by aerosol type using cluster analysis and Gobbi coordinates

Objective 6: to study the time-dependent dispersal of aerosol clusters worldwide by tracking spatial variations in characterized ANN-derived AMP on global maps for a number of climatologically and/or socio-economically important cases

Objective 7: to produce accurate, daily-updated, global maps of AMP characterised by aerosol type

Objective 8: to test the accuracy and feasibility of creating a global near real-time monitor of aerosols and an alerting service for the assessment of climatological risks and the issuing of early-warnings.

Objective 9: to engage in science communication to inform the public of the project, its results and the potential impact of global aerosol characterisation on European Research Area (ERA) environmental policy.

The expected results (deliverables), resulting from attainment of these objectives are expected to be:

Deliverable 5: Rendering of global ANN-derived AMP maps in Gobbi coordinates

Deliverable 6: Rendering of global ANN-derived AMP maps with aerosol typing

Deliverable 7: Pilot studies of aerosol temporal variation (tracking) for a number of climatologically and/or socio-economically important cases

Deliverable 8: Production of accurate, daily-updated, global maps of AMP on a global grid of resolution 1 degree CMG

Deliverable 9: A global real-time monitor of aerosols and alerting service for the assessment of climatological risks and the issuing of early-warnings

Deliverable 10: Creation of a project website/portal and the organization by the fellow of two public open days

and will involve the following methods:

Method 3: Cluster analysis and aerosol type classification (*Objective 5*)

Method 4: Dispersion analysis (*Objective 6*) and real-time monitoring/alerting (*Objectives 7 & 8*)

Method 5: Website design and public engagement (*Objective 9*).

Finally in this section, the milestones due for this reporting period are as follows:

Milestone 3: Assessment report on the classification of aerosols and the development of the real-time monitor and online alerting service (month 18)

Milestone 4: Final report (month 24)

2.2 Work progress and achievements during the period

PHASE C: (months 9-15)

TASK C1 (months 12-15): cluster analysis of global AERONET sites

In the mid-term report, we presented the results of clustering AERONET inversion data from the period 1996-2011. There, we repeated the clustering approach used by Omar et al. (2005). Despite having a longer record of AERONET data available, the conclusion of our study was the same as Omar et al. (2005) – i.e. that 99.7% of the data (only 10 days of data were unclassified) was associated with just 6 clusters or aerosol types/mixtures (see Fig. 5a in the mid-term report). While this was an encouraging result, counting the number of days of data assigned to each cluster (see Fig. 5b of the mid-term report), we found that 3 clusters accounted for the vast majority (98.74%) of the data: cluster 1=59.25%, cluster 3=13.40%, cluster 4=26.09% (59,780/100,889, 13,518/100,889 and 26,319/100,889 respectively). Analyzing the optical and microphysical properties of these 3 dominant clusters allowed us to identify them as desert dust (cluster 1), urban SO₂ (cluster 3) and biomass burning (cluster 4). The vast source of global aerosol arising from the oceans was not identified as a high-membership cluster and this raised alarm bells. It was realised that there is a logistical problem with applying cluster analysis to AERONET Level 2 (and Level 1.5) inversion data. As mentioned in Section 2.1 of the mid-term report (under Task A1), AERONET complete inversion records are only provided when certain meteorological conditions are met such as AOD>0.4. Marine aerosol has been found to be associated with much AOD values well below this threshold (typically 0.1-0.15). Therefore AERONET sites located on islands and in coastal regions where AOD values are typically low, do not contribute data records to the clustering process. This was verified by inspection of the EXCEL file (**AERONET_global_ranked_data.xlsx** at the project website) which presents a ranking of sites by complete records of AERONET inversion data (see also Task A1 in Section 2.1 of the mid-term report) reveals this selection effect since most of the island and coastal AERONET sites are absent from the list. As such, the technical constraint (AOD>0.4) associated with AERONET inversion data meant that a different approach to cluster analysis was needed (to identify marine clusters in particular). The technical constraint described above associated with low AOD values on the provision of retrievals from the AERONET inversion

algorithm, raised doubts about the appropriateness of rendering global maps in Gobbi coordinates (expected Result 5 described in Section 2.1) - since both the fine mode geometric radius and the fine mode fraction are sensitive to accurate determination from the aerosol size distribution and the refractive index (in the Mie calculations required). As such, in a project meeting between the fellow and SIC, a decision was made to focus Task C1 on a partitioning of the global grid via aerosol mixture composition rather than attempting to infer aerosol types by isolating them from AERONET inversion data. As a result, Objective 5 was changed from:

"Objective 5: to classify and characterise the global ANN-derived AMP by aerosol type using cluster analysis and Gobbi coordinates"

to:

"Objective 5: to classify and characterise the global ANN-derived AMP by aerosol type using cluster analysis"

and Deliverable 5 was changed from:

"Deliverable 5: Rendering of global ANN-derived AMP maps in Gobbi coordinates"

to:

"Deliverable 5: Partitioning of the globe into distinct aerosol types/mixtures using cluster analysis"

Refer to Section 2.3.2 and Section 2.3.5 for more discussion on this slight deviation from the Work Plan and its negligible impact on project outcomes. After some initial tests, a methodology was developed based on: a) downscaling mean global data from the GOCART chemical model, b) performing cluster analysis and c) extracting AERONET inversions in each cluster and identifying its average aerosol microphysical and optical properties. The GOCART chemical model calculates the contribution of different types of aerosols (desert dust, sea salt, organic and black carbon, and sulphate) to the AOD. GOCART's outputs are calculated on a 2.5 x 2 degree (longitude x latitude) grid and are produced every 3 hours. For any given record, 6 world maps (the total AOD and the contribution to this total from each of the 5 aerosol types: desert dust, sea salt, organic and black carbon, and sulphate) are therefore produced. The entire GOCART data record spanning the period 01/01/2000 to 31/12/2006 (=complete 7 years of 3-hourly data) were downloaded. To align the data temporally with satellite data used by AEROMAP, daily-averages were calculated (from the mean of the 8 x 3-hourly calculated values) for each aerosol type map. Code was then written to interpolate the 2.5 x 2 degree data onto a finer 1x1 degree (latitude x longitude) grid (the same spatial resolution as the satellite products used as NN inputs). The global mean (downscaled) GOCART extinction AOD <EAOD> for the period 2000-2006 (inclusive) is shown below:

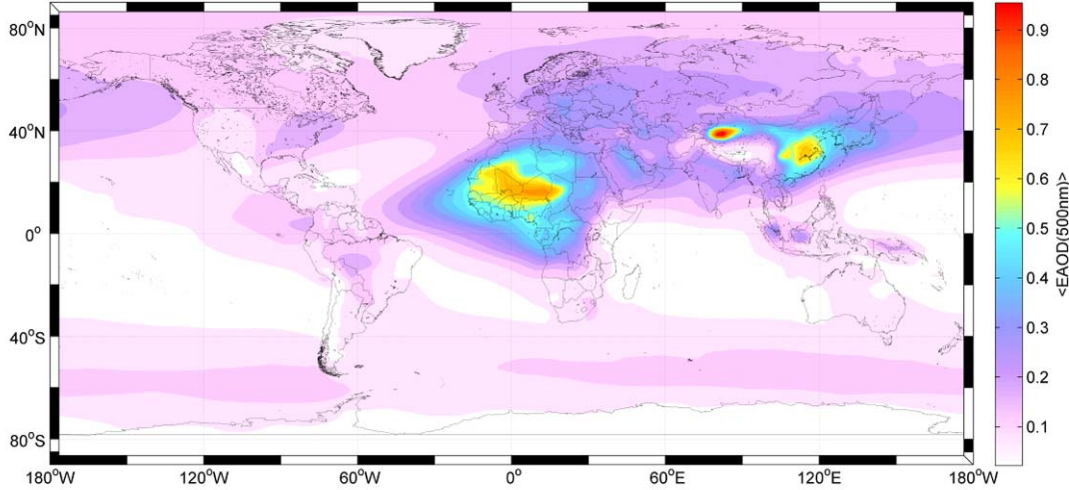


Fig. 1. Global mean (downscaled) GOCART extinction AOD $\langle \text{EAOD} \rangle$ calculated from 3-hourly values spanning the period 01/01/2000-31/12/2006.

Fig. 1 shows that the regions of peak mean global aerosol loads (associated with the EAOD) are over the Sahara and Nigeria in Northern Africa, in the Gobi desert to the north of the Himalayas and over a large region centred on Beijing. By aerosol type/chemistry, the global mean (downscaled) GOCART black carbon (BC), organic carbon (OC), biomass burning smoke (BB=BC+OC), sulphate (SU), dust (DU) and marine sea salt (SS) AOD contributions (as a percentage) are shown below:

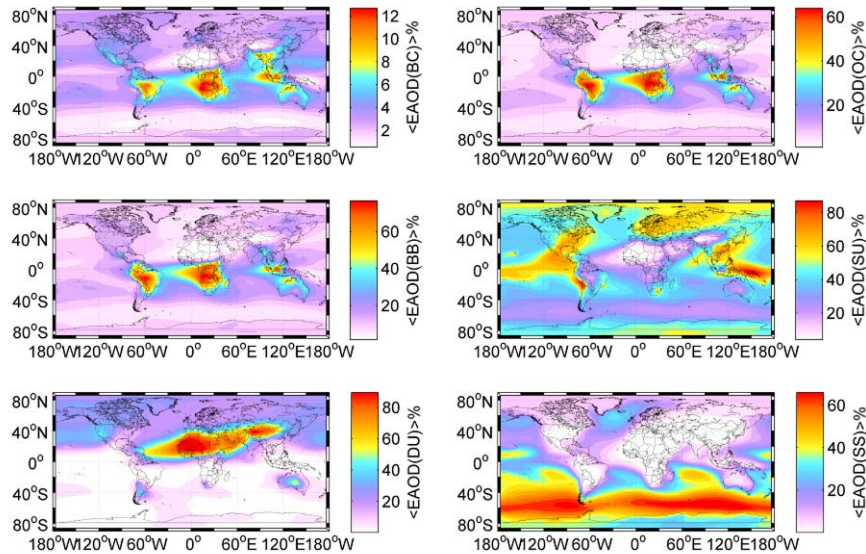


Fig. 2. Global mean (downscaled) GOCART EAOD contribution from black carbon (BC), organic carbon (OC), biomass burning smoke (BB=BC+OC), sulphate (SU), dust (DU) and marine sea salt (SS) as a percentage calculated from 3-hourly values spanning the period 01/01/2000-31/12/2006.

The largest contributions to the mean global AOD are from dust and sulphate (the colour bar axis extend to nearly 100%). Dust is seen to occupy an extended (and slightly inclined) band about 30 degrees latitude in height between 10-40°N and approximately 180 degrees longitude in extent. Marine sea salt aerosol appears to be confined strongly in the Southern hemisphere and its peak occupies a narrow band about 20-30 degrees latitude in height (situated around 60°S) and extends across the globe in longitude. Black carbon aerosol has a smaller percentage contribution to the overall EAOD (<15%) and is strongly co-located with organic carbon. This is because BC and OC are both biomass burning (BB=BC+OC) aerosol products and explains the occurrence of their peak contributions over the Amazon forest, in the African Savannah and the forests of Borneo and Indonesia. The contribution of sulphate is more dispersed. Peaks are observed

over Indonesia and Santiago (Chile) but strong contributions are clearly visible at Mexico City, the North East coast of the USA, Japan, the Eastern coast of China, and the whole of Europe (with the exception of the southern periphery).

Having downscaled the GOCART data, the next task was to perform cluster analysis on the global distribution of the 4 aerosol types: BB, SU, DU and SS. Mathematically, this is a 6-D problem involving the 6 variables: latitude, longitude, %BB, %SU, %DU and %SS. In order to perform cluster analysis, it was necessary to convert the maps shown in Fig. 2 into a single matrix. This was achieved by “unfolding” each map. The maps are each a 180 (rows/latitude) x 360 (columns/longitude) matrix whose elements are the percentage contribution of the relevant aerosol type. Unfolding the map involves converting each of the map matrices into a 64800 (rows) x 3 (column) matrix as follows. The number of rows comes from the fact that a 180 x 360 matrix contains 64800 cells or pixels. Since each pixel has its own latitude and longitude together with the percentage contribution, each row therefore has 3 entries. Unfolding the mean global GOCART maps in this way allowed us to construct a matrix that combines all of the available data, i.e. we could construct a single matrix having 64800 rows and 6 columns: latitude, longitude, %BB, %SU, %DU and %SS. Cluster analysis could then be applied to the last 4 columns of this matrix to partition the global grid into aerosol mixtures (one for each cluster). To achieve this, a k-means clustering algorithm was coded in MATLAB that calculated the sum of the Euclidean distances (“energy”) from each cluster centre to every point in the 4-D space of percentage contributions contributing to that cluster. To mitigate the effect of centres being confined to local minima, the initial cluster centres were chosen randomly. This was repeated 10 times with the centres and the energy being stored each time. The lowest energy case of the 10 trials was then retained as the best clustering. This entire procedure was repeated stepping through 1 to 18 cluster centres. The variation of the energy (E) with the number of clusters is shown below:

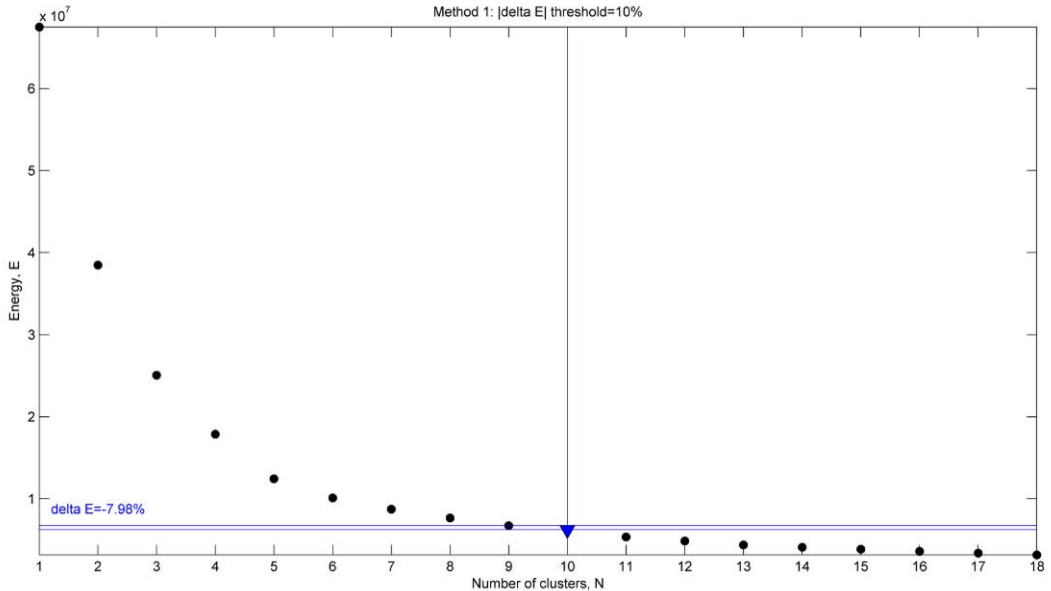


Fig. 3. The variation of the sum of Euclidean distances (energy, E) with the number of clusters, N applying the k-means algorithm to the matrix of mean global GOCART contributions of BB%, SU%, DU% and SS%. Note that for each N , 10 random centre seeds were used and the best case selected.

This approach led to a smoothly decaying variation of E with N . As per Omar et al. (2005), the optimal number of clusters was detected with the condition that the change in energy (ΔE) fell below 10% of the initial energy value. This corresponded to $N=10$ clusters. As an independent check on the validity of the $\Delta E < 10\%$ condition, we devised two other stopping conditions. The first is based on the number of “half-lives”. The curve of Fig. 3, when plotted on log-log (natural logarithm) axes, was found to be strongly fit by a linear regression (especially for $N>4$). This told us that the improvement of the clustering with the number of clusters followed an exponential decay. The linear fit in log-log space was used to find the location of the

values of N corresponding to consecutive halving of E. In this space, these points lie at equally-spaced distances along the best fit line as shown by the red triangles in the figure below:

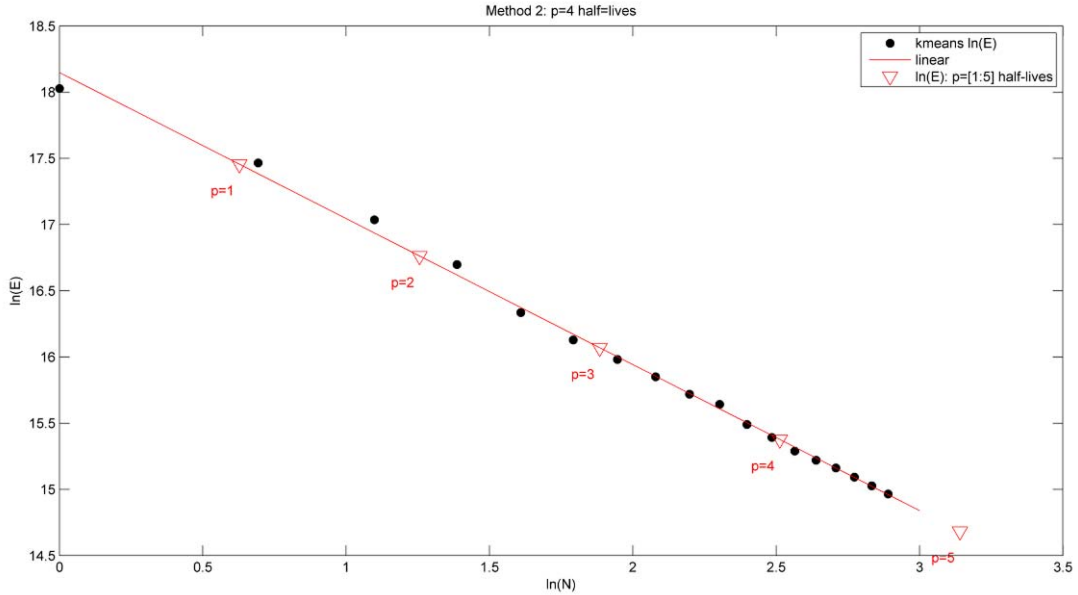


Fig. 4. The variation of $\ln(E)$ with $\ln(N)$ is strongly fit by a straight line suggesting that the energy follows an exponential decay law with increasing number of clusters. The values of $\ln(E)$ corresponding to $p=[1,..,5]$ "half-lives" are overlaid.

In order to find lower and upper bounds for the optimal number of clusters, we analysed the results of using different numbers of half-lives, p . In each case, the point (N, E) closest to the value of $\ln(E)$ corresponding to each value of p then allowed for determination of $\ln(N)$ and hence the optimal number of clusters. For $p=3$ half-lives, the optimal number of clusters is $N=6$ (i.e. closest to the 6th black point along the best fit line in Fig. 4). The change in energy from the previous point ($N=5$) to this point ($N=6$), i.e. $\Delta E \gg 10\%$ and suggests that $p=3$ is a lower bound on the optimal number of clusters. For $p=4$ half-lives, the optimal number of clusters is $N=12$ (i.e. closest to the 12th black point along the best fit line in Fig. 4). With reference to Fig. 3, ΔE is clearly $< 10\%$ here and thus $N=12$ is an upper bound on the optimal number of clusters. This method suggests that the optimal number of clusters N is between 6 and 12, in agreement with our first method above using $\Delta E < 10\%$ as a stopping condition. We therefore adopted $N=10$ as the optimal number of clusters.

The k-means cluster algorithm then associates each row in the unfolded matrix (i.e. each pixel) with one of the 10 clusters. Our task then was to visualize the result. We decided to follow as closely as possible the colour scheme used for aerosol types by the CALIPSO LIDAR aerosol retrieval algorithm: black=smoke, red=pollution, yellow=dust, blue=marine and green=rural. In our case, each cluster corresponds to a mean aerosol *mixture* – containing a combination of BB, SU, DU and SS. The closest parallel is to make the following associations: BB="smoke" and colour-code it black, SU="pollution" and colour-code it red, DU="dust" and colour-code it yellow, and SS="marine" and colour-code it blue. This scheme also has the desirable property that these are primary colours and are visually perceptible to all (i.e. they do not create ambiguities in perception due to colour-blindness for example). With this colour-coding, the cluster analysis with $N=10$ optimal clusters gives rise to the following stacked bar chart of mean aerosol mixtures:

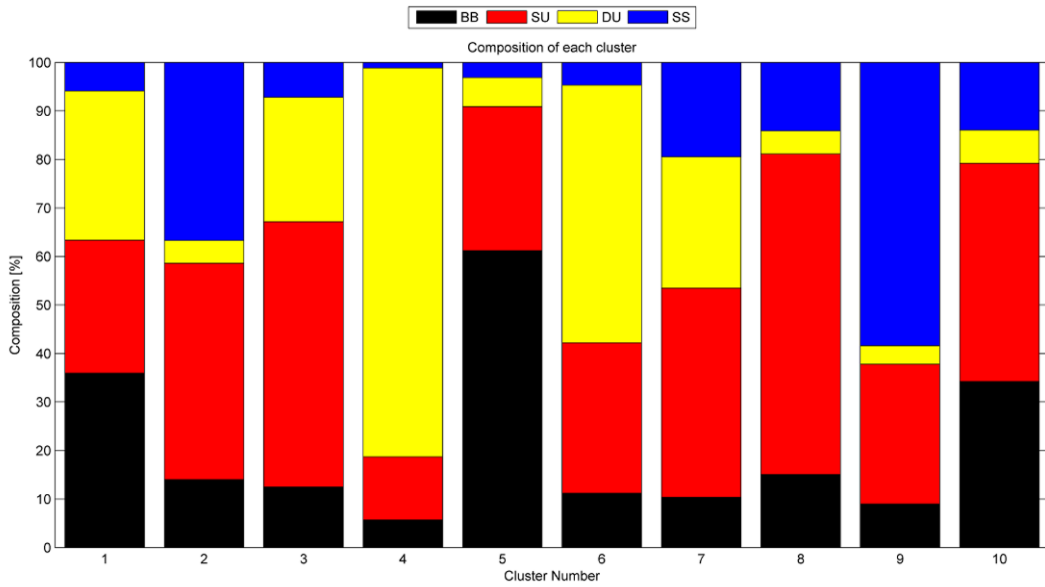


Fig. 5. The aerosol composition of each cluster resulting from application of the k-means algorithm and the stopping condition to the mean global GOCART AOD percentage contribution data.

Note that cluster 4 is DU-dominated, cluster 5 is BB-dominated, cluster 8 is SU-dominated and cluster 9 is SS-dominated. All other clusters (1,2,3,6,7 and 10) are not clearly dominated by a single aerosol type. Our next task was to produce a global map of the clusters to see how they are spatially distributed worldwide. A challenge here again was the use of colour and creation of a scheme suitable for representing mixtures of aerosols. In order to retain a visual link with the colours assigned to pure aerosol types (BB=black, SU=red, DU=yellow and SS=blue), for each cluster we simply mixed these primary colours in accordance with the percentage of each aerosol type assigned to each cluster. As a further visual point of reference, we added a colour key to the map for both the pure types, for 50%:50% mixtures of any 2 pure types and for each cluster with its mix of 4 types. The resulting global distribution of aerosol mixtures (clusters) is shown below:

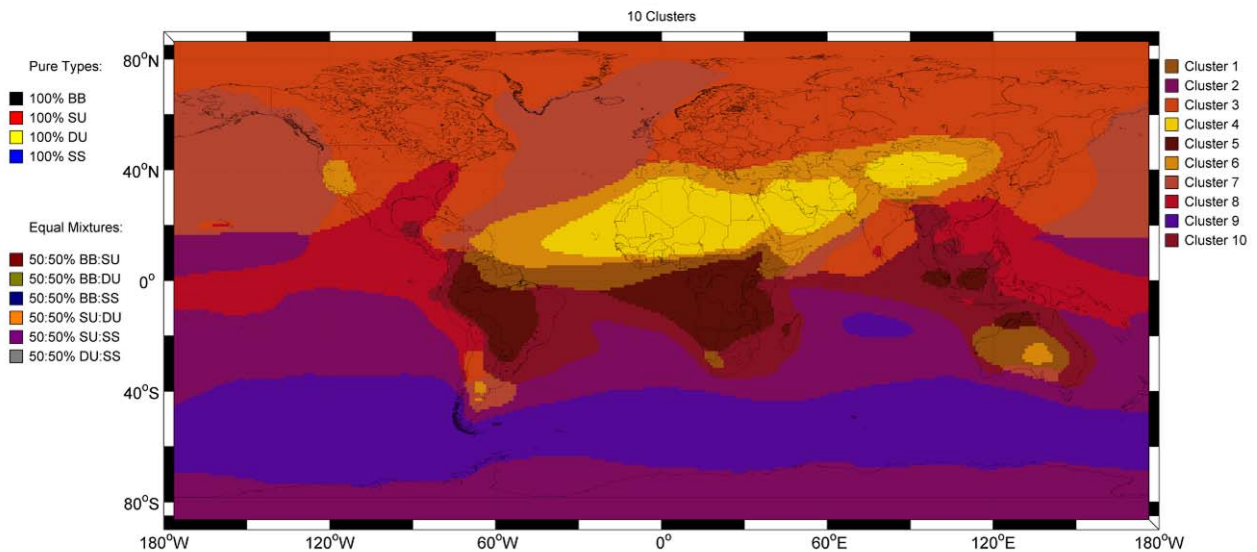


Fig. 6. The spatial distribution of aerosol types/mixtures resulting from application of the k-means clustering algorithm to the mean of global GOCART chemical data spanning the period 2000-2006 (inclusive). Note that colours are produced by mixing black, red, yellow and blue in direct proportion to the percentage contribution of each pure aerosol type (BB, SU, DU and SS) in each cluster.

The spatial occupation of clusters is shown below:

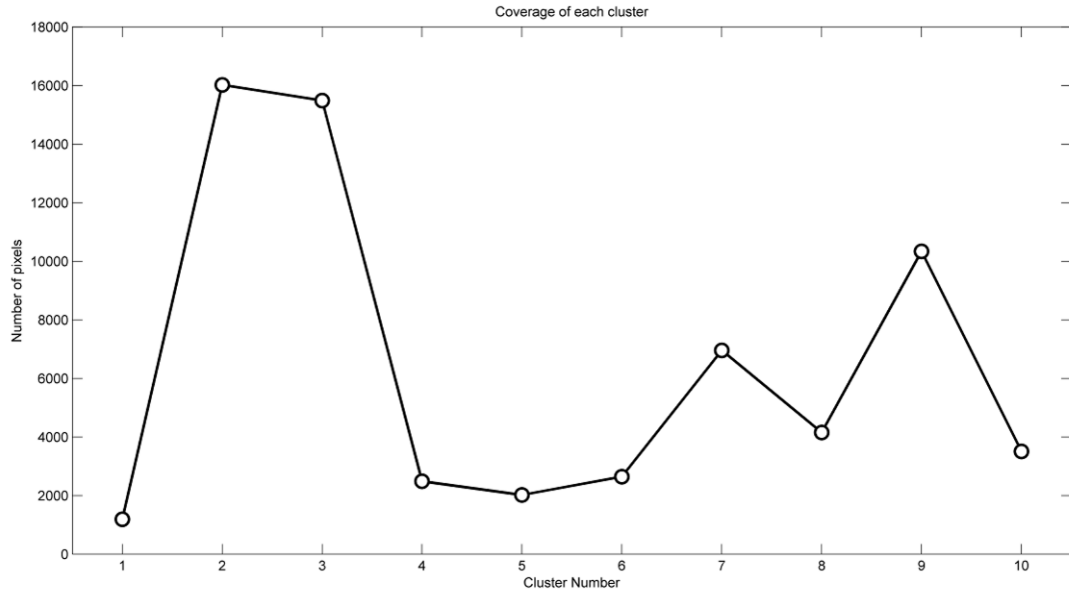


Fig. 7. The global spatial coverage of each cluster as measured by the number of pixels in the 360×180 (longitude x latitude) grid they occupy.

Clusters 2 and 3, despite not having a clear dominant aerosol type component (see Fig. 5), occupy the largest spatial extent and fill the most pixels of the global grid. Clusters 2 and 9 (“sulphurous marine” aerosol) together span the southern oceans (below about 15°S) while clusters 3 and 7 (“dusty sulphate” aerosol) together span the northern hemispheric region (above about 15°N). This new methodology was able to achieve the required partitioning of the globe into distinct aerosol types/mixtures and a manuscript is in preparation to be submitted to the *Journal of Atmospheric Chemistry and Physics*.

To assess the effect of seasonal/climatological trends, we extracted GOCART model chemical data according to month of the year and grouped the data into 3-month triplets: December + January + February (DJF), March + April + May (MAM), June + July + August (JJA), and September + October + November (SON) as shown for the global mean AOD in Fig.8 below:

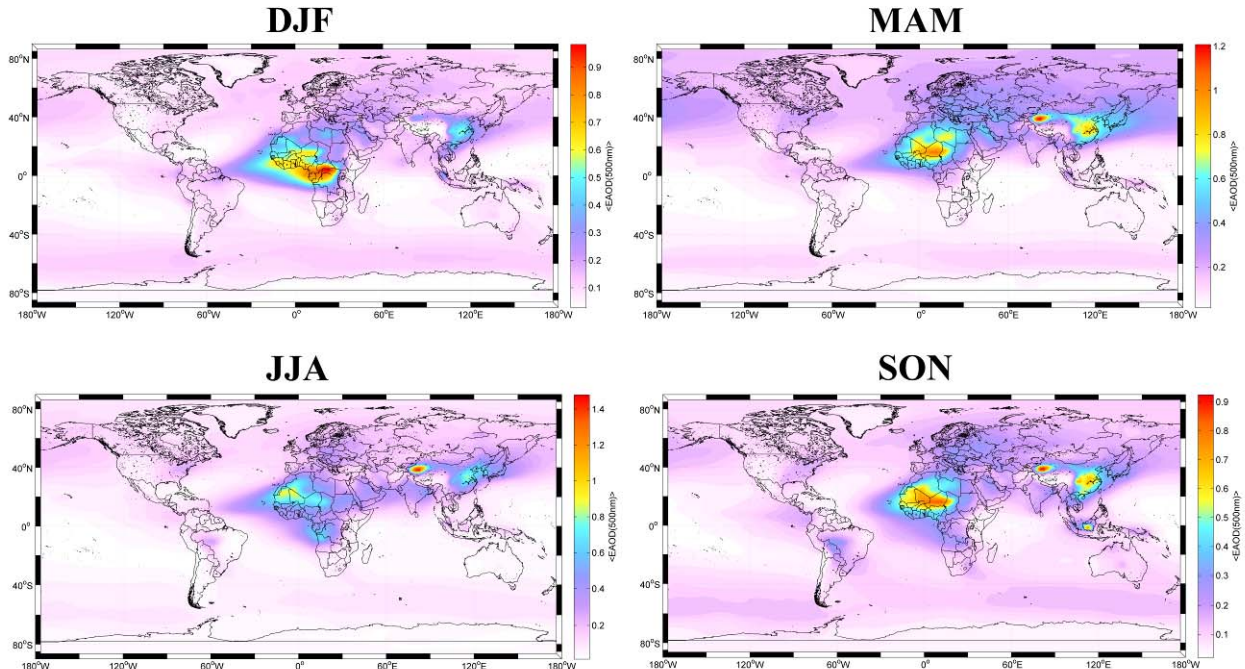


Fig. 8. Global seasonal mean (downscaled) GOCART extinction AOD $\langle\text{EAOD}\rangle$ calculated from extracted 3-hourly values in the 3-month triplets DJF, MAM, JJA and SON spanning the period 01/01/2000-31/12/2006.

There are some noticeable but small differences in the spatial distribution of the mean AOD. The main sources of aerosol, while exhibiting some seasonal variation in intensity, are largely located in the same spatial locations. To assess whether or not similar trends were observed in the corresponding aerosol type/mixtures, we performed cluster analysis on the seasonal GOCART data. Fig. 9 shows that, despite a small variation in the number of clusters identified (10-12 clusters), the salient features of the spatial distribution of aerosol type/mixtures are seen to be largely similar:

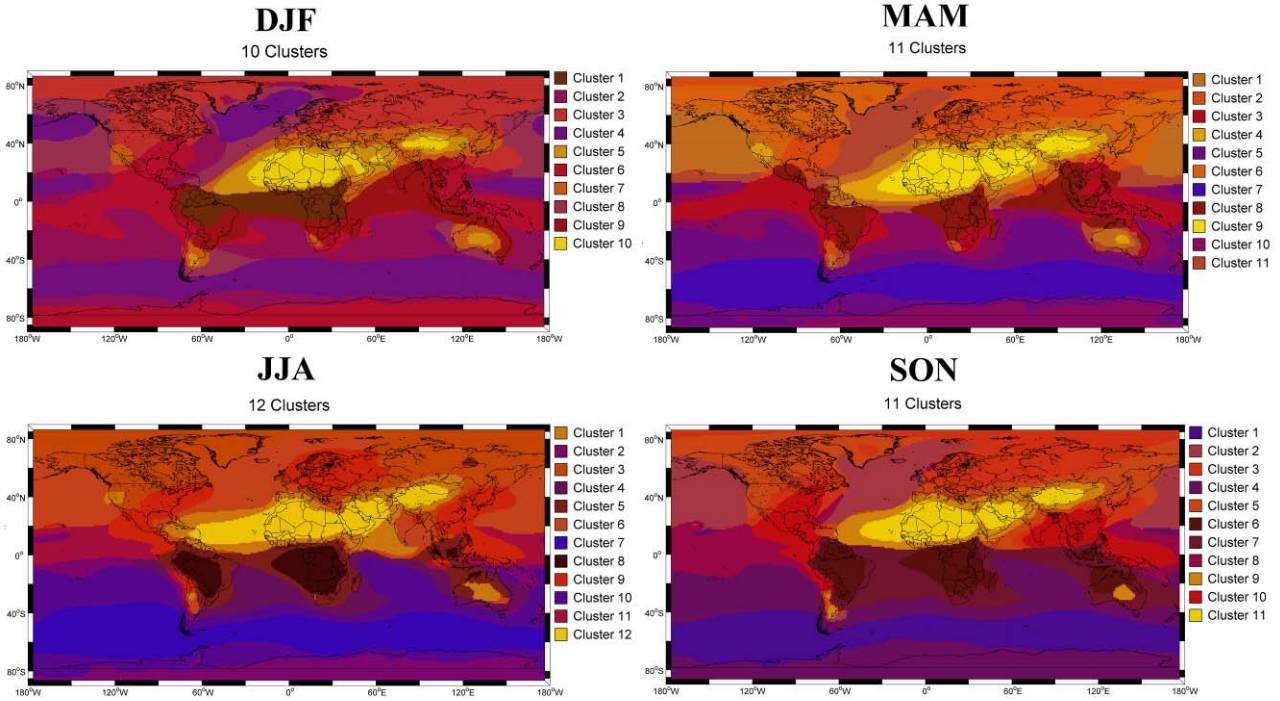


Fig. 9. The spatial distribution of aerosol types/mixtures resulting from application of the k-means clustering algorithm to the seasonal mean of global GOCART chemical data spanning the period 2000–2006 (inclusive). Note that colours are produced by mixing black, red, yellow and blue in direct proportion to the percentage contribution of each pure aerosol type (BB, SU, DU and SS) in each cluster.

This motivated us to retain the 10-cluster partition obtained with the global mean of the entire GOCART record (Fig. 6). In order to satisfy Objective 5 with this method, for each cluster we extracted AERONET inversion data and calculated descriptive statistics for aerosol parameters as follows. The complete record of AERONET “all points” inversion products from 01/03/1993-31/12/2013 containing a total of 715,288 records from 969 sites was downloaded. On any given day, the data record of inversion products for a given site is not homogeneous due to the quality assurance criteria implemented in the Level 2.0 Version 2 product (see Periodic Report 1 for details). The plot below shows the inhomogeneity in the AERONET inversion data record as a function of aerosol parameter:

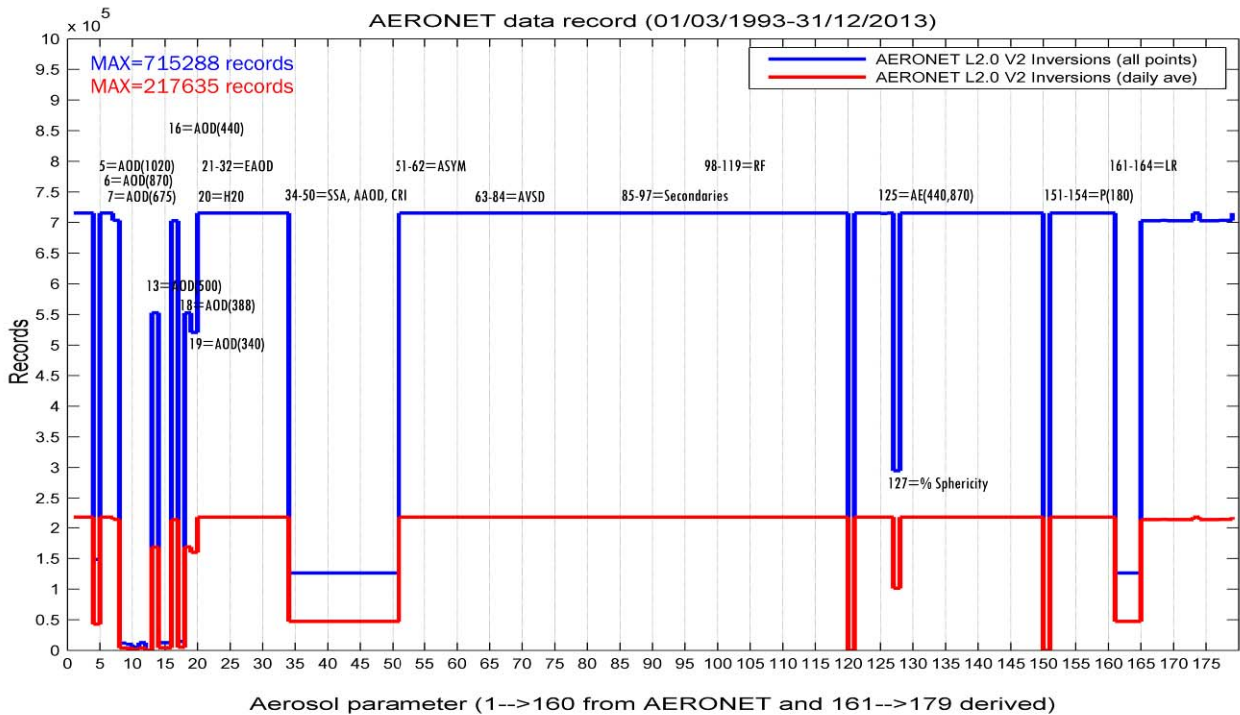


Fig. 10. The number of AERONET L2.0 Version 2 inversion retrieval records for each of 179 aerosol parameters. The blue line shows the distribution of “all points” records with parameter and the red line shows the distribution of “daily-averaged” records (calculated from the “all points” records). Key parameters are indicated.

Complete (100%) data records of AERONET Level 2.0 Version 2 inversions are provided for: AOD(1020), AOD(870), H₂O, ASYM(λ), AVSD(22 bins) together with its secondary parameters, and the phase function at 180 degrees P(180). The AOD(675) and the AOD(440) comprise 98.35% and 98.24% respectively of the available data record and this translates into a 98.24% provision of extrapolated AOD(470), AOD(550) and AOD(660) due to the impact of the former on Angstrom Exponent value availability. Note also that AOD(500), AOD(380) and AOD(340) data is only provided by the newer CIMEL sun photometers and hence contribute to a smaller fraction of records (77.25%, 77.20% and 72.79% respectively). There are also several other AOD measurements that contribute to an extremely low fraction (< 2%) of records: parameters 8=AOD(667), 9=AOD(555), 10=AOD(551), 11=AOD(532), 12=AOD(531), 14=AOD(490), 15=AOD(443) and 17=AOD(412). Note that parameters 120 and 150 are two text flags and contain no numerical data and therefore contribute zero numerical records. Parameters that are sensitive to aerosol absorption (the SSA, AAOD and CRI) comprise only 17.63% of the record and have a corresponding data compression effect on parameters that are derived from them (e.g. LIDAR ratios). Similarly, the %sphericity contributes to only 41.22% of record. It is clear then that inclusion of any of these parameters in NN models leads to data loss. Furthermore, for temporal alignment with the satellite data record, we calculated daily-averages directly from the “all points” data. The number of daily-averages is 30.43% of the number of “all points” records. The impact of data inhomogeneity and daily-averaging translates to a 93.39% loss of the maximum number of “all points” data for records that include any of the absorption parameters (SSA, AAOD and CRI). Having, extracted all daily-averaged, homogeneous AERONET records (i.e. having no missing data), we then calculated descriptive statistics for each parameter including the mean and standard deviation, and also the median and inter-quartile range for each cluster. As an illustration, Figs. 11-13 below show descriptive statistics of the AVSD, aerosol microphysical parameters (AMPs) and aerosol optical parameters (AOPs) for the mean of the AERONET record in the dust-dominated cluster 4 and the biomass burning-dominated cluster 5:

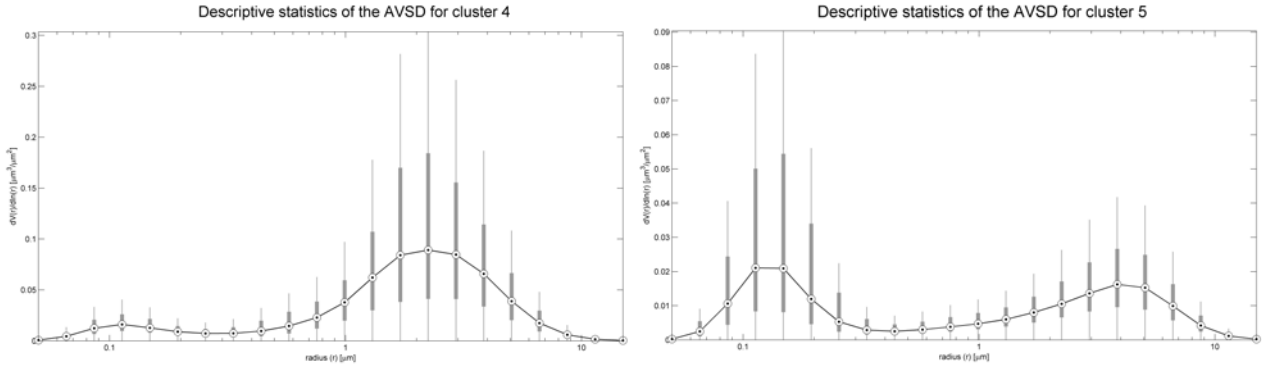


Fig. 11. The median, inter-quartile range (IQR) and outlier (median ± 1.5 IQR) statistics of the AVSD for cluster 4 (“desert dust”) and cluster 5 (“biomass burning”). Note the enhanced coarse mode of cluster 4 and the strong fine mode of cluster 5.

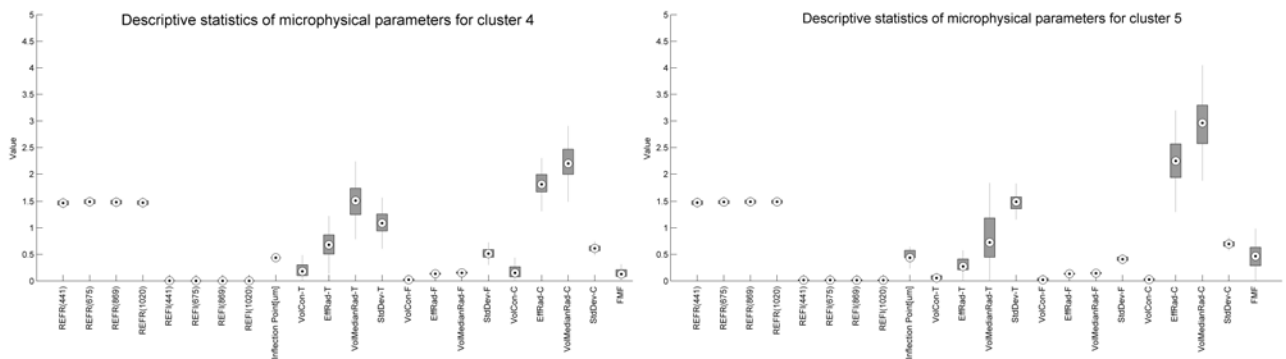


Fig. 12. The median, inter-quartile range and outlier statistics of the aerosol microphysical parameters for cluster 4 (“desert dust”) and cluster 5 (“biomass burning”). On this scale, the differences in the refractive index real part (REFR) and imaginary part (REFI) are almost imperceptible. Significant differences are observed between clusters 4 and 5 particularly in the following parameters: the volume concentration of the coarse mode (VolCon-C), the total volume (VolCon-T) and the geometric median radius of the coarse mode (VolMedianRad-C). The former two translate into a substantial difference in the fine mode fraction (FMF).

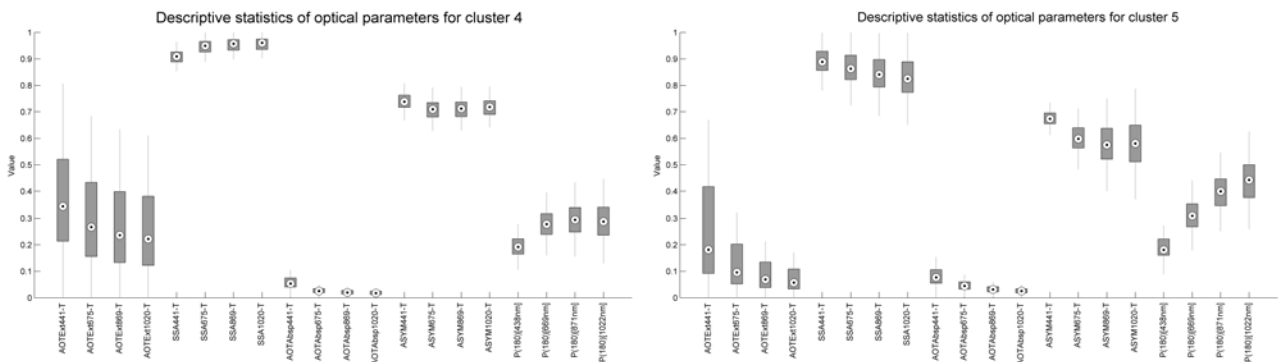


Fig. 13. The median, inter-quartile range and outlier statistics of the aerosol optical parameters for cluster 4 (“desert dust”) and cluster 5 (“biomass burning”). Note the very different spectral behaviour of each of the parameters in each of the two clusters. For example, the SSA of dust shows an increase with wavelength while that of biomass burning shows a decrease with wavelength.

The cluster averages obtained from the mean values of the AERONET record extracted in each cluster allowed us to generate the first mean global maps of AOPs and AMPs (a selection of parameters is illustrated in Figs. 14 and 15 below):

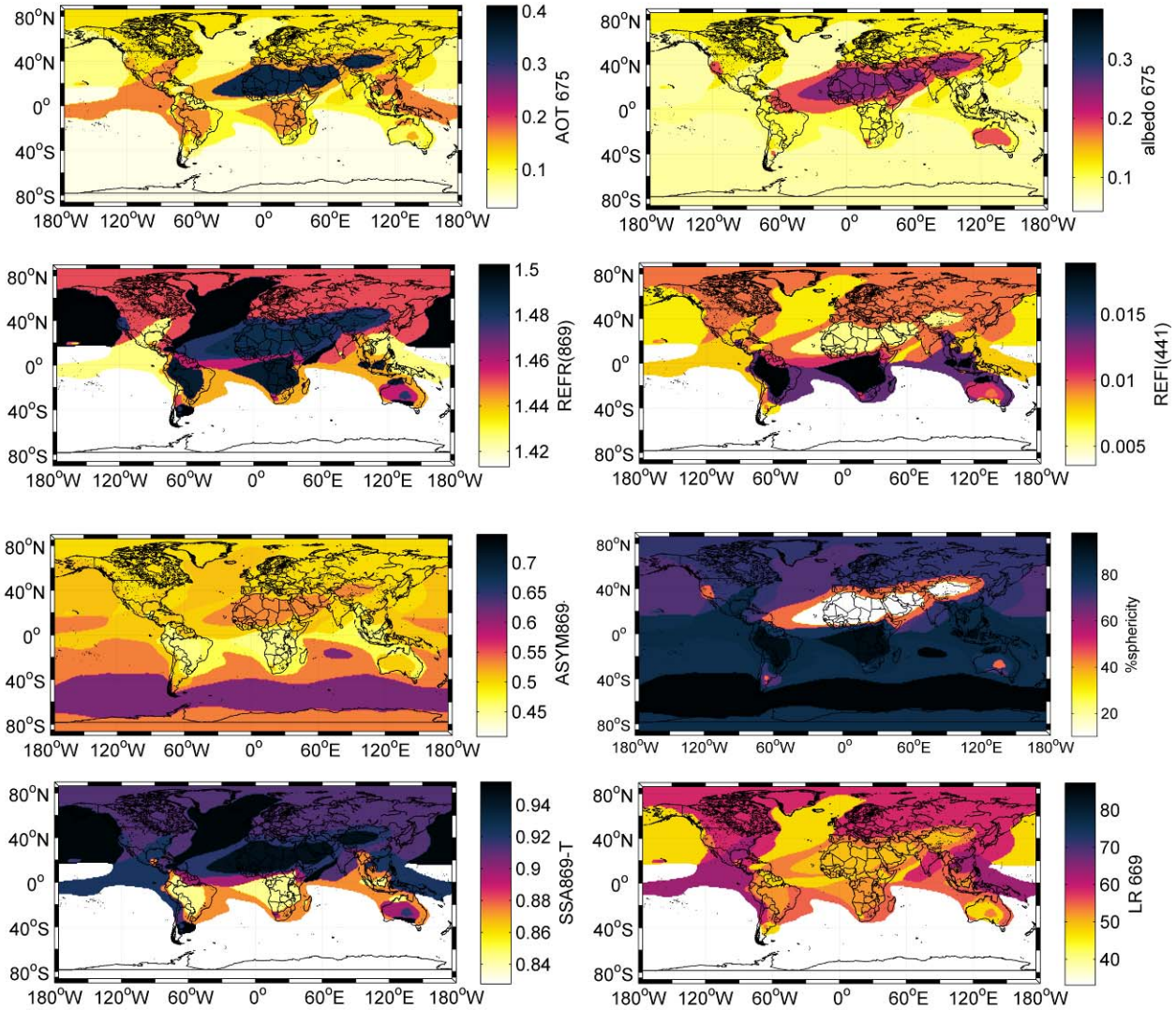


Fig. 14. Global mean cluster values of extracted AERONET AOPs and AMPs.

Fig. 14 shows that over the period 2000-2006 (inclusive), the mean aerosol load as represented by the aerosol optical thickness ("AOT") has, as expected, its peak in the dust-dominated region of cluster 4 (see also Fig. 1 and Fig. 2). High loads are also seen in the biomass burning-dominated region of cluster 5 and also the polluted sulphate-dominated region of cluster 8. The northern hemisphere generally presents high aerosol loads whereas the southern hemisphere oceans present relatively low aerosol loads. A similar picture is reflected also by the surface albedo. The imaginary part of the refractive index ("REFI"), which correlates strongly with absorption, shows that biomass burning aerosol regions and their periphery as well as in the sulphate polluted northern hemisphere are strongly absorbing. Desert dust is weakly absorbing. Note also that, due to the low values of the AOT, AERONET's inversion algorithm does not retrieve REFR, REFI, SSA over the southern oceans. In terms of scattering properties, backscattering asymmetry is strongest for the sea salt peak centred on 50°S and is generally high over the southern oceans. While these zones show a high presence of spherical particles (most likely due to the presence of sulphates originating from petroleum mining in Patagonia), the dust belt comprises highly non-spherical aerosol in the atmospheric column. The SSA map, reinforces the picture painted with regard to desert dust – that, while asymmetric, it is strongly reflecting (i.e. non-absorbing). The dolphin-shaped region of high SSA in the Atlantic is possibly associated with the transport of such aerosol into this region where it is trapped in the vortex north of the Gulf stream. Conversely, lower SSA values are observable in the biomass burning-affected regions and the sulphate-dominated region of the northern hemisphere – suggesting the presence of strongly absorbing particles in these global zones. Finally here, while AERONET obtains an averages value

over the light path sampling the atmospheric column, LIDAR ratios can be estimated from the back-scattered part of the phase function $P(180^\circ)$ and the SSA via the expression: $LR = 4\pi / SSA \times P(180^\circ)$. LR therefore scales with $1/SSA$ and hence is directly proportional to the non-back-scattered component (i.e. the absorbing component). As a result, it echoes the qualitative features observed in the map of REFI. In order to show the global mean AVSD, Fig. 15 below shows the secondary microphysical parameters derived from it: the volume concentration of the fine mode ("VolCon-F") & coarse mode ("VolCon-C") together with the median radius of the fine mode ("VolMedianRad-F") & coarse mode ("VolMedianRad-C"):

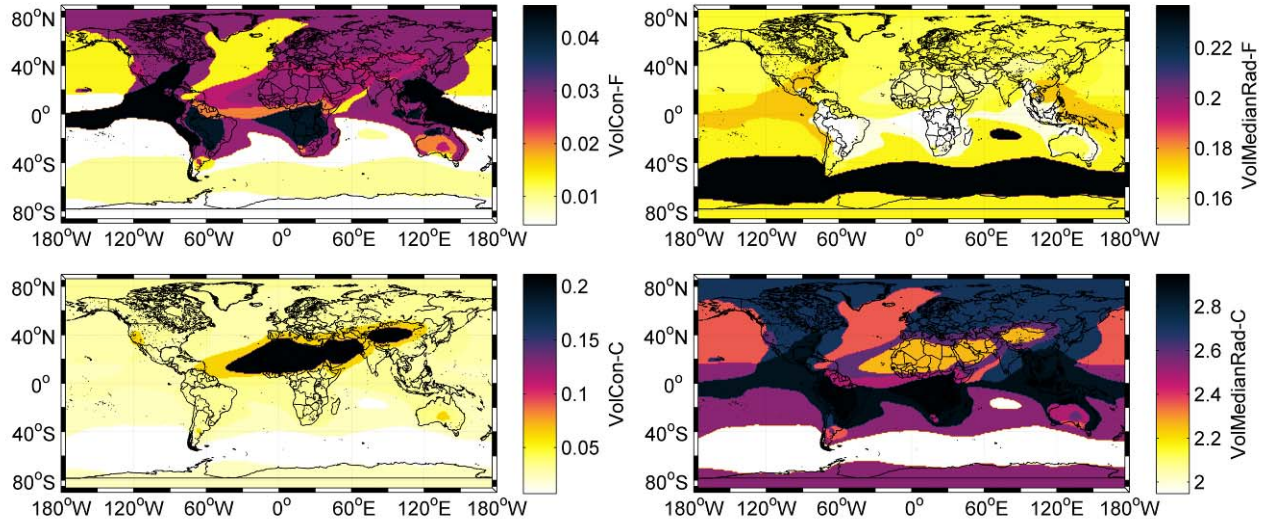


Fig. 15. Global mean cluster values of secondary microphysical parameters derived from extracted AERONET AVSD mean values in each cluster.

Fine particles clearly dominate biomass burning-dominated regions and their periphery. However they are also predominant in dust regions and the sulphate-dominated north hemisphere. The median ("geometric") radius of fine aerosol is highest in the sea salt band centred on 50°S and lowest in biomass burning-dominated regions and their periphery. Of interest is the observation that fine dust has a slightly lower median radius than the surrounding aerosol type/mixture regions. Coarse particles, as expected, dominate in the dust region and its periphery and present their lowest concentration in the sea salt band where their median radius is also lowest. Interestingly the median radius of coarse particles is highest in biomass burning-dominated regions and their periphery.

TASK C1 was completed by the end of month 15 (3 months later than scheduled) due to the failure of the planned AERONET-based approach using the clustering method of Omar et al (2005). The independent approach developed in Task C1 produced a new methodology for partitioning the global grid into aerosol mixtures and for characterizing global AOP and AMP mean values. Task C1 satisfied Objective 5 and its main outcome was Deliverable 5:

Deliverable 5: Partitioning of the globe into distinct aerosol types/mixtures using cluster analysis.

TASK C2 (months 12-18): pilot studies

The first application of the results of the clustering analysis described above was in the context of dust retrievals over the Sahara. The lower right panel of Fig. 14 shows that the LIDAR ratio (LR) for the dust-dominated cluster is in the mid-50s. However, this is at odds with values reported in the literature for the Sahara which suggested lower values of the LIDAR ratio in the low 40s. This finding led the fellow to contribute directly to a LIDAR consortium research article on optimization of Saharan dust retrievals from the Cloud–Aerosol Lidar and Infrared Pathfinder Satellite Observations (CALIPSO) as co-author. The work demonstrated improvements in CALIPSO dust extinction retrievals over northern Africa and Europe when corrections are applied to the Saharan dust LIDAR ratio. In particular, it was found that application of a

universal, spatially-constant LIDAR ratio of 58sr instead of 40sr to individual CALIPSO Level 2 dust-related backscatter products produced AODs that showed an improvement compared with both synchronous and collocated AERONET measurements and MODIS measurements:

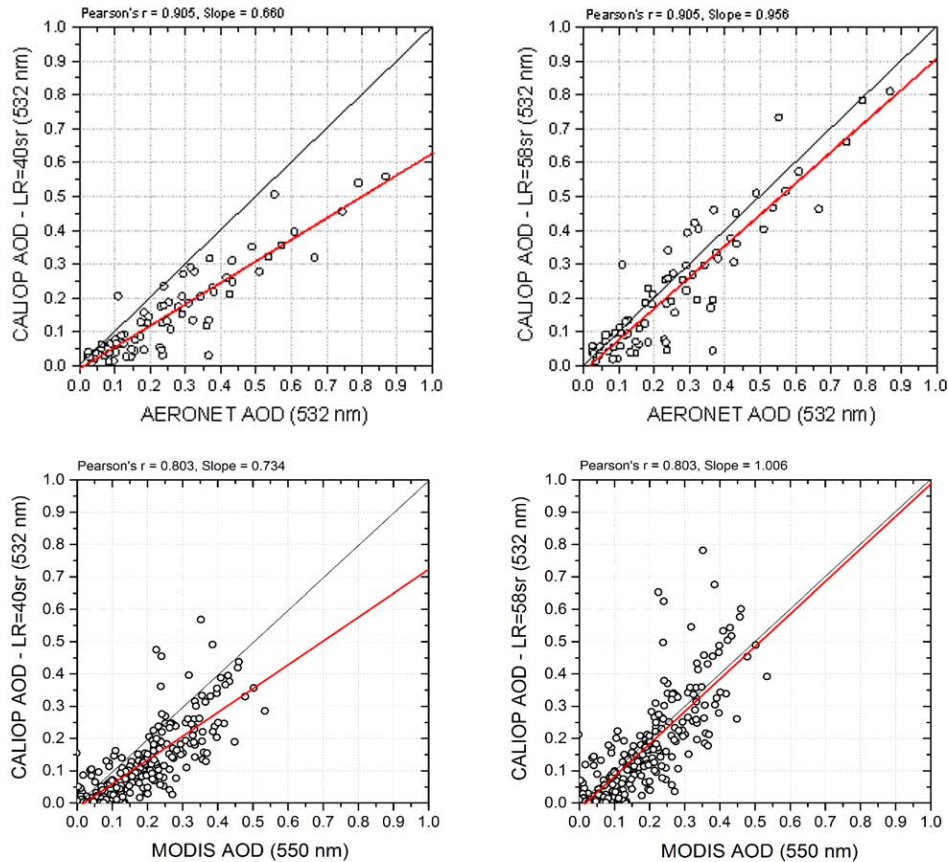


Fig. 16. Upper Panels: Scatter plot comparison of CALIPSO AOD vs. co-located AERONET measurements when LR is equal to 40 sr (left) and when LR is equal to 58 sr (right). Lower Panels: Comparison of CALIPSO AODs (1 × 1 degree) vs. co-located MODIS-Aqua Level 3 using LR equal to 40 sr (left) and LR equal to 58 sr (right).

When compared with AERONET the absolute bias was found to be of the order of -0.03 (improving on the statistically significant biases of the order of -0.10 reported in the literature for the original CALIPSO product), and when compared with the MODIS collocated aerosol optical depth (AOD) product, the CALIPSO negative bias is even less. The article was published in the high-impact factor *Journal of Atmospheric Chemistry and Physics*.

Bi-Product: Co-authorship of a research article now published in a high-impact factor journal:

Amiridis, V., Wandinger, U., Marinou, E., Giannakaki, E., Tsekeri, A., Basart, S., Kazadzis, S., Gkikas, A., Taylor, M., Baldasano, J., & Ansmann, A. (2013). Optimizing Saharan dust CALIPSO retrievals. *Atmospheric Chemistry and Physics* 13, 12089-12106.

The second pilot study based on observation of this interesting anomaly associated with Saharan dust involved us using the dust-dominated cluster 4 to extract sites to test and validate NNs developed in Phase C. Central to this endeavour was the use of the cluster analysis of Task C1 to spatially-isolate and extract AERONET sites contributing dust-dominated aerosol shown in Fig. 17:

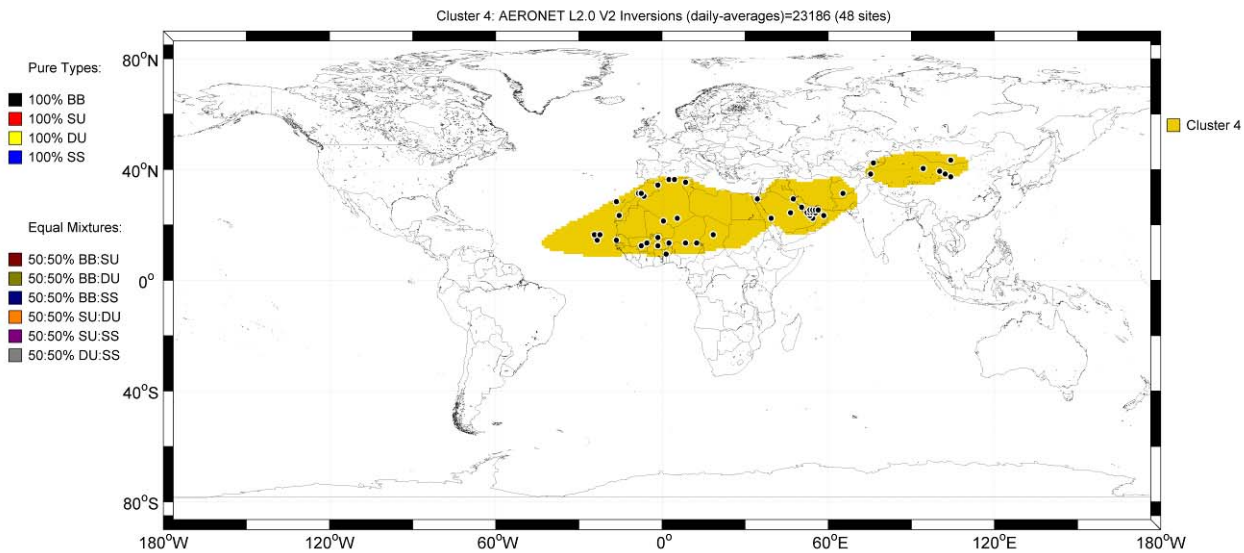


Fig. 17. The 48 AERONET sites contributing 23,186 full records of inversion products in the dust-dominated cluster 4.

A targeted sub-set of 7 dust-dominated ($>84.8\%$) sites (shown below in Fig. 18) lying on the peak of the dust AOD (according to GOCART) were then selected as a test bed to train and validate the spatial extrapolation potential of an neural network constructed to convert satellite inputs to AERONET inversion outputs:

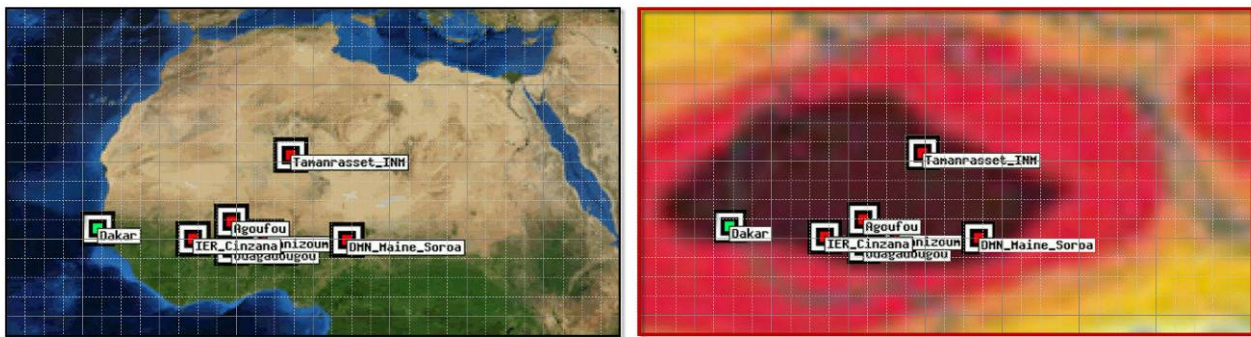


Fig. 18. The 48 AERONET sites contributing 23,186 full records of inversion products in the dust-dominated cluster 4. Left: A satellite map showing the location of the 6 Northern African (NAF) AERONET sites used to train the NN models (red) and the Dakar (green) site used for NN testing. Right: An overlay of the same sites on the peak of dust AOD for the study region extracted from GOCART.

The NNs were trained with satellite measurements as input variables and co-located and synchronous AERONET microphysical and optical parameters as the target output variables, and were then validated with unseen AERONET data. Until now, estimates of aerosol properties from space have made use mainly of look-up tables to match aerosol properties to corresponding light measurements on a case by case (and day by day) basis. The NN calculation of the inverse function (between satellite inputs and AERONET outputs) may require considerable time due to the need for run and optimize a grid of trained NN models (see below) but, once complete, the NN solution is instantaneous and simultaneously retrieves target output variables in a single step – without having to re-calculate each day. Such NN retrieval schemes therefore (potentially) have the capacity to produce real-time retrievals for large datasets on the global scale. This study drew on four different data sources. Satellite inputs comprising over eight years of daily measurements (2004–2013) of the AOD at 470, 550, 660nm and the columnar H₂O from the MODIS Aqua Level 3 Collection 5.1 together with the absorption AOD at 500nm from the Ozone Measuring Instrument (OMI) Level 3 OMAERUV algorithm were derived at a spatial resolution of 1×1 degree. In conjunction with

this, co-located (in the same pixel) and synchronous daily-averaged ground-based target outputs including the AVSD retrieved in 22 logarithmically-equidistant radial bins spanning the range of particle radii from 0.05 to 15 μm , the real and imaginary parts of the CRI(λ), the SSA(λ) and the asymmetry parameter ASYM(λ) centred at $\lambda = 440, 675, 870$ and 1020 nm were then extracted from the AERONET Level 2.0 Version 2 inversion algorithm.

As described in Periodic Report 1, our approach is based on NN models since feed-forward NNs, having at least one layer of intermediary neurons whose activation functions are nonlinear hyperbolic tangent (*Tanh*) functions or sigmoidal functions, have been proved to operate as universal function approximators. This means that given enough neurons and training data, such NNs are (potentially) capable of learning the numerical relation between satellite inputs and output aerosol parameters. We developed a new automated procedure to detect the optimal architecture based on permuting the number of intermediary neurons and the proportion of data used for training (t%), and then selecting the NN having the lowest mean squared error MSE between network outputs and AERONET targets. NNs having Tanh activation functions, and learning by back-propagating errors with the Levenberg-Marquardt algorithm, were coded in MATLAB script and the optimal trained NN was found by: 1) normalizing all input and output variables, 2) applying principal components analysis (PCA) to inputs and outputs separately to exclude redundant variability, 3) looping through a grid of 100 NNs of varying numbers of hidden neurons (4–24 neurons in steps of 2) and proportions of training data (40–90% in steps of 5 %), and 5) selecting the NN having the minimum MSE between its outputs and the target AERONET outputs. A schematic of the learning process is shown in Fig. 19. The number of co-located (satellite-ground) and synchronous (daily) complete available NAF AERONET records used to train the NN were 139 days, and 169 days of complete co-located and synchronous records at Dakar were used to test the optimal NN.

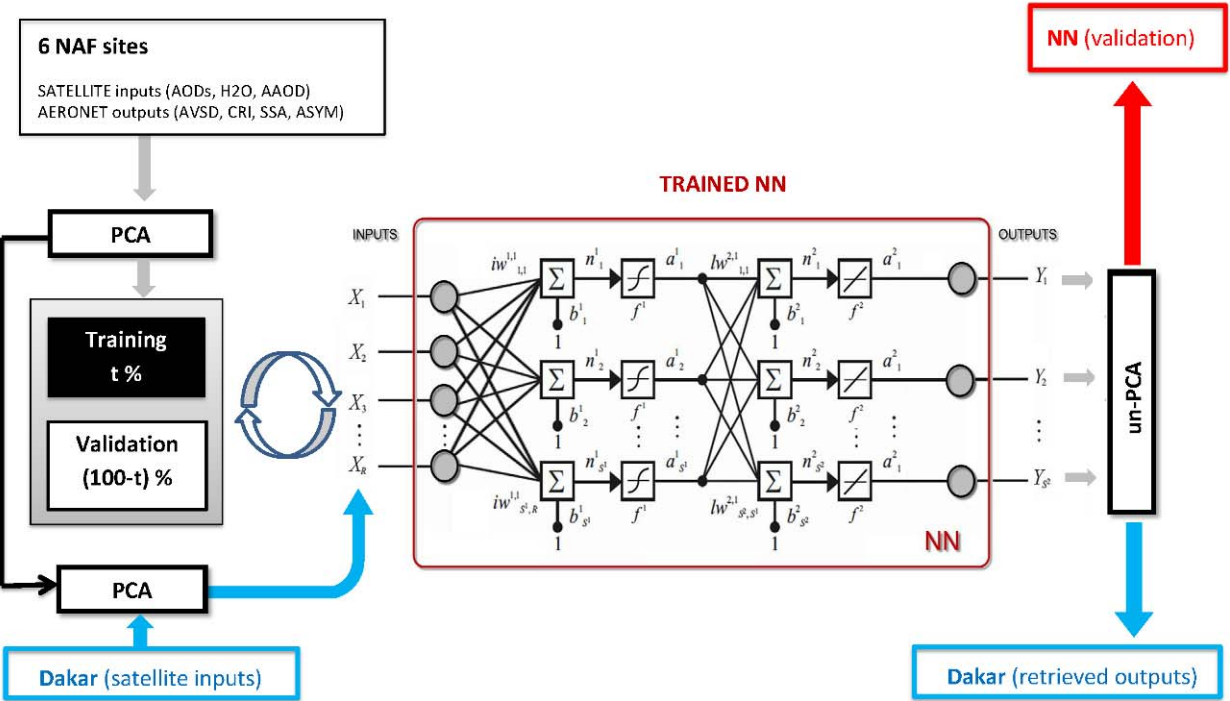


Fig. 19. A schematic of the modeling process. PCA is applied to co-located and synchronous, normalized satellite inputs and AERONET outputs from 6 North Africa (NAF) sites and the PCs are used to train each NN in a grid of 100 NN architectures (varying t% and number of neurons) until the MSE between NN PC outputs and PC target outputs is minimized. Real-space outputs of the optimal NN are obtained by transformed back with reverse principal components (“un-PCA”). To test the optimal trained NN, new (“unseen”) satellite inputs at Dakar are presented to the optimal trained NN and used to retrieve daily co-located and synchronous aerosol parameters.

The optimally-trained NN was able to retrieve the magnitude of aerosol parameters (their mean values) but also importantly their variability on the daily timescale – required in order to attain Objectives 7 and 8 and to provide Deliverable 9. As an illustration, Fig. 20 below shows the NN retrieval of SSA(440) obtained from satellite inputs over Dakar as compared with collocated and synchronous daily-averaged values obtained by AERONET:

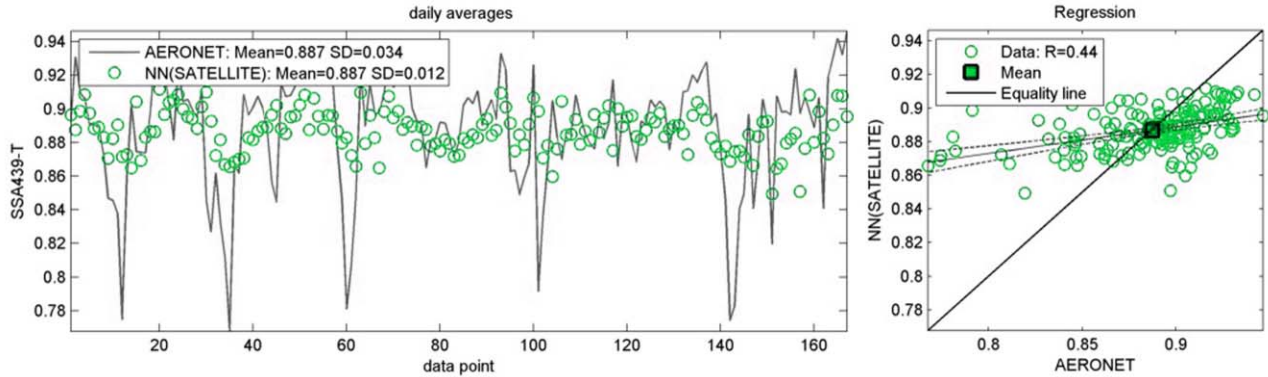


Fig. 20. The retrieval of the daily-averaged SSA at Dakar using the NN trained on input-output data at 6 sites in the vicinity.

The mean of the NN retrieval of this parameter and the AERONET retrieval are equal to 3 decimal places. Note that the NN model also simultaneously retrieves the SSA together with the AVSD, the CRI and ASYM parameters. An analysis of the number of NN retrievals that fall within the suggested levels of acceptable uncertainty are shown in Table 1 below:

	Aerosol Parameter	Uncertainty (Mishchenko et al 2007)	<AERONET>	<NN>	N Certain	% of sample falling within the uncertainty limits
Microphysics	$r(f)$	±10%	0.115	0.118	102	60.40%
	$r(c)$	±10%	1.928	1.909	58	34.30%
	$var(f)$	±40%	1.529	1.514	169	100.00%
	$var(c)$	±40%	3.056	2.65	169	100.00%
	CRI-R(440)	±0.02	1.472	1.457	66	39.10%
	CRI-R(675)	±0.02	1.488	1.479	76	45.00%
	CRI-R(870)	±0.02	1.472	1.471	76	45.00%
	CRI-R(1020)	±0.02	1.459	1.46	70	41.40%
Optics	SSA(440)	±0.03	0.901	0.897	124	73.40%
	SSA(675)	±0.03	0.948	0.947	115	68.10%
	SSA(870)	±0.03	0.954	0.957	119	70.40%

Table 1. Uncertainty analysis using the target levels of Mishchenko et al. (2007). Results are shown for unseen satellite inputs at Dakar on the daily timescale fed to an optimal NN having 22 intermediary neurons, trained on 90% of the NAF data and validated on the remaining 10%.

While the width (variance) of the fine and coarse modes in the AVSD is certain and the mean radius of the fine mode is found with some 60% certainty, the mean radius of the coarse mode is of low certainty. The daily SSA retrieval is excellent but the CRI is retrieved with moderate ($\approx 40\%$) certainty.

	$V(f)$	Poor		SSA(440)	Good
	$V(c)$	Very Good		SSA(675)	Moderate
	η	Good		SSA(870)	Moderate
	Radial Bin 15	Good		SSA(1020)	Moderate
Microphysics	CRI-R(440)	Moderate	Optics	ASYM(440)	Very Poor
	CRI-R(675)	Poor		ASYM(675)	Very Poor
	CRI-R(870)	Poor		ASYM(870)	Very Poor
	CRI-R(1020)	Poor		ASYM(1020)	Very Poor
	CRI-I(440)	Moderate	ASSESSMENT		
	CRI-I(675)	Moderate			
	CRI-I(870)	Moderate			
	CRI-I(1020)	Moderate			

Fig. 21. Our overall assessment of the potential of the NNs to spatially-extrapolate at the daily timescale.

In the case of the spatially-extensive Saharan desert region, our NN retrievals were found to be generally good for the AVSD, moderately accurate for the SSA, but poor for the CRI and ASYM parameters. The study of Saharan dust allowed us to validate that NN models could be constructed to retrieve AMPs on the daily timescale over an extensive region (Northern Africa). This work led to publication of a peer-reviewed research article:

Bi-Product: Lead authorship of a research article published in a high-impact factor journal:

Taylor, M., Kazadzis, S., Tsekeri, A., Gkikas, A., Amiridis, V. (2013). Satellite retrieval of aerosol microphysical and optical parameters using neural networks: a new methodology applied to the Sahara desert dust peak. *Atmospheric Measurement Techniques Discussions* 6, 10955-11010, 2013.

Bi-Product: Lead authorship of a conference paper contributing to the proceedings of an important international conference on atmospheric physics, climatology and meteorology:

Taylor, M., Kazadzis, S., Tsekeri, A., Gkikas, A., Amiridis, V. (2014). AEROMAP: Satellite retrieval of dust aerosol microphysical and optical parameters using neural networks. *Proc. 12th Int. Conf. on Meteorology, Climatology and Atmos. Phys. (COMECAp)*, 28-31/05/2014, Heraklion, Crete, Greece. (under review).

The fellow's expertise on deduction of secondary microphysical parameters from the AVSD aerosol size distribution meant that he was invited by the SIC to participate in data processing, analysis and interpretation of measurements of aerosol microphysics produced by the World Meteorological Organisation's precision filter radiometer (PFR), and their comparison with AERONET retrievals. The algorithms and visualisation tools that the fellow had developed in Tasks B3, C1 and the present Task C2 were readily applied to the PFR data and the outcome was co-authorship on a consortium paper led by the SIC:

Bi-Product: Co-authorship of a research article published in a high-impact factor journal:

Kazadzis, S., Veselovskii, I., Amiridis, V., Gröbner, J., Suvorina, A., Nyeki, S., Gerasopoulos, E., Kouremeti, N., Taylor, M., Tsekeri, A., Wehrli, C. (2014). Aerosol microphysical retrievals from Precision Filter Radiometer direct solar radiation measurements and comparison with AERONET. *Atmospheric Measurement Techniques Discussions* 7, 99-130, 2014.

In the post-12 month phase of Task C2, attention was focused on novel features observed in the AVSD of dominant aerosol types which suggested that the standard bi-lognormal fit to the size distribution used by

AERONET's inversion algorithm, was inaccurate - and hence could have a large negative impact on the calculation of secondary microphysical parameters like the fine mode fraction and the fine and coarse mode geometric radii and volume concentrations being produced by the NNs. In a project meeting, a decision was made to investigate ways to improve the fit to the size distribution so that these important parameters could be more accurately determined. Inspired by an approach used by atmospheric chemists to produce mass distributions, and with the collaboration of Dr Evangelos Gerasopoulos (the director of the host group and an expert in atmospheric chemistry), the fellow developed a new technique using Gaussian mixture models to fit the AVSD with multiple modes ($n>2$). Fig. 22 shows the method being used to fit the AVSD of dominant marine aerosol at Lanai at Hawaii on the 21nd of January 2002:

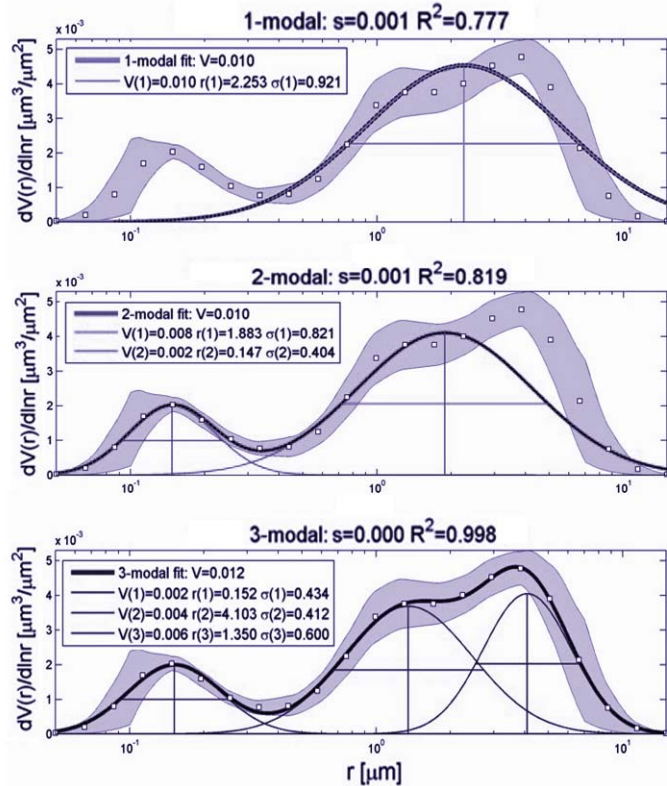


Fig. 22. Gaussian mixture model fits of the AVSD for dominant marine (sea salt) aerosol at Lanai, Hawaii on the 21st of January, 2002. The grey shaded region is the error on the AERONET data and the black dotted lines (most visible in the 5 and 6-modal plots) are the 95% confidence level curves on the fit.

The method also greatly improved the fit to the AVSD (and hence deduction of secondary microphysical parameters) for another strongly atypical (non-bilognormal) and newly-reported case of fog-induced aerosol modification at Fesno, USA on the 11th of February 2006:

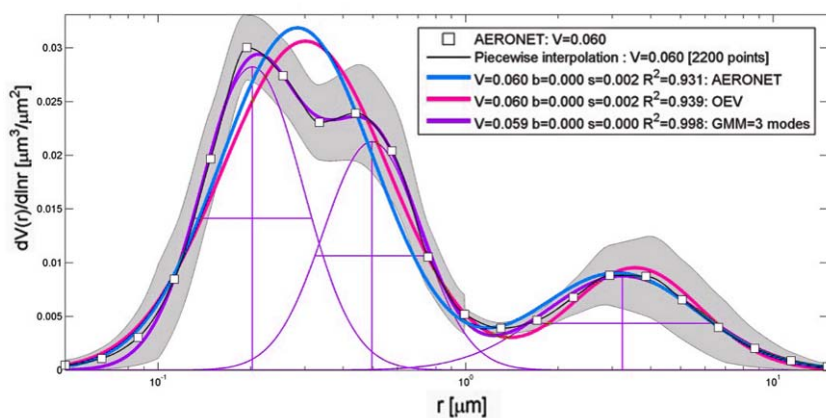


Fig. 23. Comparison of the interpolated AVSD, the AERONET bi-lognormal fit, the OEV bi-lognormal fit and the GMM optimal fit for the daily-averaged AERONET AVSD at Fresno on the 11th of February, 2006 which displays a clear double-hump in the fine mode region. The grey band is the uncertainty on the AERONET AVSD.

Application of the method to dust, biomass burning, urban sulphate and marine aerosol-dominated AVSDs in Task C2 led to two further publications:

Bi-Product: Lead authorship of a research article published in a high-impact factor journal:

Taylor, M., Kazadzis, S., Gerosopoulos, E. (2013). Multi-modal analysis of aerosol robotic network size distributions for remote sensing applications: dominant aerosol type cases. *Atmospheric Measurement Techniques Discussions* 6, 10571–10615, 2013 (in press at AMT).

Bi-Product: Lead authorship of a conference paper contributing to the proceedings of an important international conference in the field:

Taylor, M., Kazadzis, S., Gerosopoulos, E. (2014). Multi-modal fitting of AERONET size distributions during atypical aerosol conditions. *Proc. 12th Int. Conf. on Meteorology, Climatology and Atmos. Phys. (COMECAp)*, 28-31/05/2014, Heraklion, Crete, Greece. (under review).

Furthermore, the method was applied to the temporal evolution of aerosol mixtures during high load aerosol events including: a desert dust storm, a savannah wildfire outbreak, an urban pollution cloud formation and the impact of volcanic ash at a coastal site. A manuscript has been prepared for submission to the *Journal of Atmospheric Chemistry and Physics* which presents these findings. This ongoing work will contribute to other aspects of the European research effort on environmental quality since European policy-makers have an interest in the impact for example of desert dust or urban pollution on historical sites.

Bi-Product: Lead authorship of a research article being submitted to a high-impact factor journal:

Taylor, M., Kazadzis, S., Gerosopoulos, E. (2014). Multi-modal analysis of aerosol robotic network size distributions for remote sensing applications II: temporal evolution of high load events. *Atmospheric Chemistry and Physics Discussions* (manuscript ready for submission).

Task C2 was completed 3 months later than scheduled (i.e. in month 18 rather than month 15) but satisfied Objective 6 and provided Deliverable 7:

Deliverable 7: Pilot studies of aerosol temporal variation for a number of climatologically and/or socio-economically important cases.

Importantly, Task C2 led to 6 important publications strengthening the fellow's CV and contributing also to Phase E2 on dissemination of results.

TASK C3 (months 15-18): Production of global maps

The 10-cluster partition of the global grid was used to train 10 NNs (one for each cluster i.e. aerosol type/mixture). For this task, it was necessary to obtain a homogeneous set of synchronous and co-located satellite input data and AERONET inversion output data. Global, daily gridded (1x1 degree) satellite inputs over eight years of measurements (2004-2013) were obtained from the MODIS Aqua Level 3 Collection 5.1 and the Ozone Measuring Instrument (OMI) Level 3 OMAERUV algorithm. MODIS inputs spanned the date range: 4th of April 2002 to the 16th of April 2012. OMI inputs spanned the date range: 1st of October 2004 to the 14th of December 2013. As such it was also necessary to align (i.e. seek synchronous values) the MODIS

and OMI data records. In conjunction with this, co-located (in the same pixel) and synchronous daily-averaged ground-based target AVSDs retrieved in 22 logarithmically-equidistant radial bins spanning the range of particle radii from 0.05 to 15 μm were extracted from the AERONET Level 2.0 Version 2 inversion product record spanning the period: 01/03/1993-31/12/2013. Table 2 below shows the number of homogeneous records of synchronous and co-located satellite inputs and AERONET AVSD outputs extracted for each of the 10 clusters:

SATELLITE inputs	Cluster 1	Cluster 2	Cluster 3	Cluster 4	Cluster 5	Cluster 6	Cluster 7	Cluster 8	Cluster 9	Cluster 10	ALL
1=MODIS H2O (above cloud)	2015	973	60684	24282	7070	36734	3460	13250	261	6676	155405
2=MODIS H2O (to cloud)	2015	973	60684	24282	7070	36734	3460	13250	261	6676	155405
3=MODIS H2O (column mean)	2015	973	60684	24282	7070	36734	3460	13250	261	6676	155405
4=MODIS Corrected-land AOD(470)	736	217	44162	6503	5809	26982	1716	9607	150	5839	101721
5=MODIS Corrected-land AOD(550)	736	217	44162	6503	5809	26982	1716	9607	150	5839	101721
6=MODIS Corrected-land AOD(660)	736	217	44162	6503	5809	26982	1716	9607	150	5839	101721
7=MODIS Effective-ocean AOD(470)	736	586	15970	5028	655	9318	1859	3813	15	524	38504
8=MODIS Effective-ocean AOD(550)	736	586	15970	5028	655	9318	1859	3813	15	524	38504
9=MODIS Effective-ocean AOD(660)	736	586	15970	5028	655	9318	1859	3813	15	524	38504
10=MODIS Effective-ocean AOD(870)	736	586	15970	5028	655	9318	1859	3813	15	524	38504
11=MODIS Effective-ocean AOD(1240)	736	586	15970	5028	655	9318	1859	3813	15	524	38504
12=MODIS Effective-ocean AOD(1640)	736	586	15970	5028	655	9318	1859	3813	15	524	38504
13=MODIS Effective-ocean AOD(2130)	736	586	15970	5028	655	9318	1859	3813	15	524	38504
14=OMI AAOD(388)	1322	374	35761	17822	4135	25357	1585	6949	97	4085	97487
15=OMI AAOD(500)	1322	374	35761	17822	4135	25357	1585	6949	97	4085	97487
16=OMI AOD(388)	1264	264	33687	16243	3901	24067	1427	6528	91	3913	91385
17=OMI AOD(500)	1264	264	33687	16243	3901	24067	1427	6528	91	3913	91385
18=OMI SSA(388)	1264	264	33687	16243	3901	24067	1427	6528	91	3913	91385
19=OMI SSA(500)	1264	264	33687	16243	3901	24067	1427	6528	91	3913	91385
20=OMI Al-UV	1523	843	44514	19077	4739	27875	2588	8784	141	4685	114769
21=MODIS Deep Blue AOD(470)	736	124	11293	1463	429	7108	702	2200	3	443	24501
22=MODIS Deep Blue AOD(550)	736	124	11293	1463	429	7108	702	2200	3	443	24501
23=MODIS Deep Blue AOD(660)	736	124	11293	1463	429	7108	702	2200	3	443	24501
3,4,5,6 = H2O + Land & Ocean AOD(470,550,660)	736	217	44085	6484	5789	26934	1715	9560	150	5837	101507
3,4,5,6,15 = H2O + Land & Ocean AOD (470,550,660) + AAOD(500)	389	138	26387	4644	3160	16749	968	4999	81	3307	60822
3,4,5,6,20 = H2O + Land & Ocean AOD (470,550,660) + Al-UV	422	158	26863	4772	3282	17076	1052	5218	91	3453	62387
14,15,16,17,18,19,20 = OMI (all)	1238	248	29737	16146	3593	23173	1291	5496	82	3536	84540

Table 2. The number of homogeneous records of synchronous (daily) co-located satellite inputs and AERONET Level 2.0 Version 2 inversion AVSD outputs. Each row results from a different combination of satellite inputs.

In Task C2, the optimized NN for data on the peak of dust AOD in Northern Africa was constructed using the combination of satellite inputs: 3,4,5,6,15 (see Table 2). As mentioned in our discussion of Task C2, the NN was able to successfully retrieve the AVSD with moderately high accuracy but other AMPs like the CRI and the AOPs were retrieved with less accuracy (see Table 1 and Fig. 21 for details). Table 2 shows that the number of homogeneous records available for NN training in each cluster is highly sensitive to the choice of satellite inputs. For example, the inclusion of OMI parameters substantially reduces the number of available records for training the marine aerosol clusters 2 and 9. Since it was necessary in this task to deliver global maps of AMPs, we focused on retrieval of the AVSD. The Saharan dust NN trained and validated in Task C2 revealed that the CRI and AOPs require satellite inputs to include a measure of aerosol absorption: i.e. the AAOD at 500nm. In Task C2 we learned that the AVSD can be retrieved with moderate accuracy from a combination of MODIS H2O and AOD inputs (without OMI inputs). This offers 3 advantages:

1. the number of homogeneous satellite input and AVSD output records in each cluster is maximized
2. the approach depends exclusively on data from MODIS
3. a single (MODIS) antenna is needed for obtaining real-time data

More importantly, the OMI AAOD at 500nm is subject to model constraints and the availability of climatological values of the SSA. The effect of this is to reduce the spatial coverage of this parameter in global pixels (this is shown in Fig. 24 below):

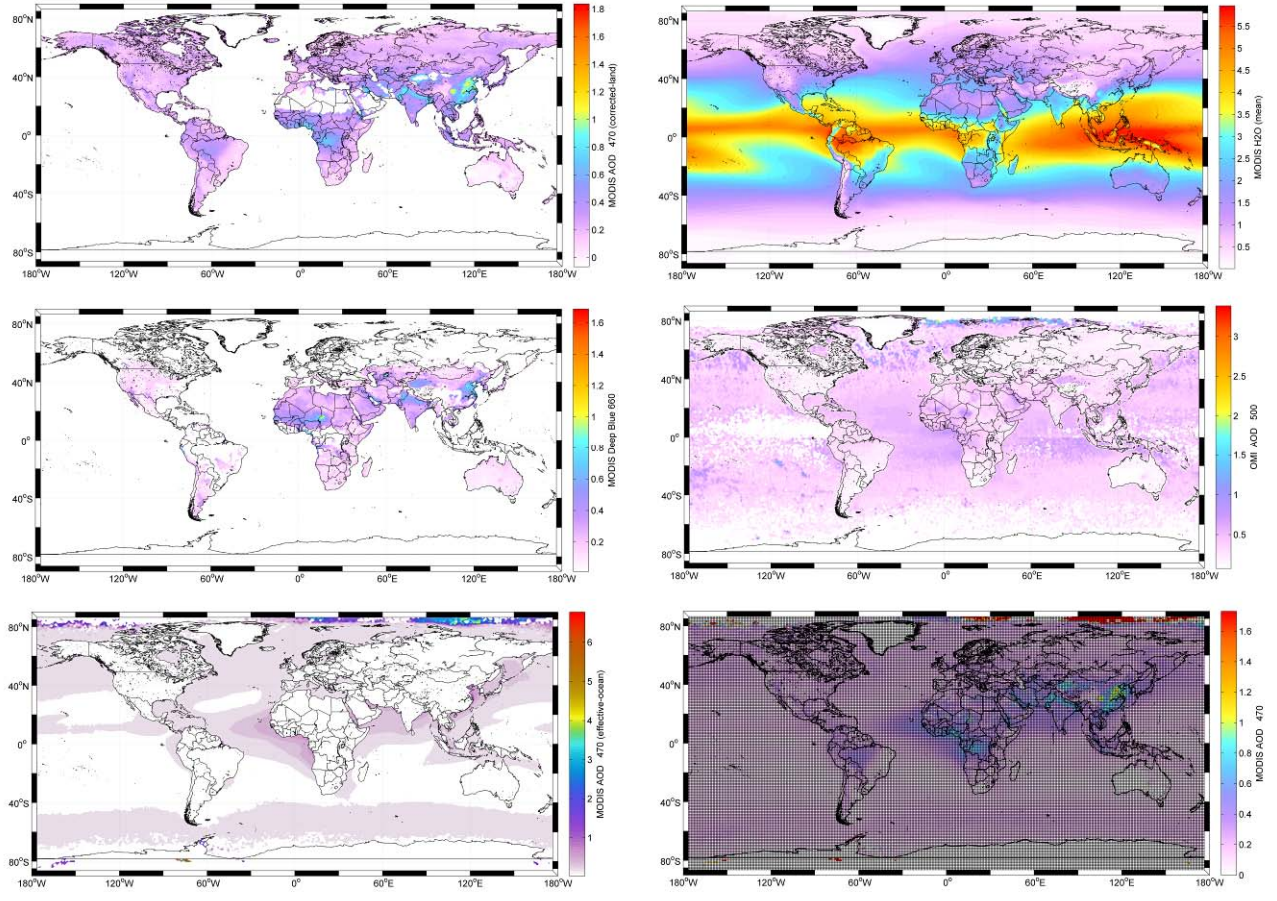


Fig. 24. Global mean map of MODIS inputs. Left upper panel: the “Corrected” AOD at 470nm over land (note the absence of data over the Sahara and central Australia). Left middle panel: the “Deep Blue” AOD at 470nm over land (‘bright surface targets’). Left lower panel: the “Effective” AOD at 470nm over ocean (‘dark targets’). Right upper panel: the mean columnar water vapour (‘H₂O’). Right middle panel: the OMI AAOD at 500nm (note the patchiness of even the 8 year mean at the global level). Right lower panel: the AOD at 470nm obtained using the pixel selection method used by AEROMAP. Note that the high surface albedo associated with snow and ice means that 4 regions of the global grid have empty pixels: the Arctic, the Antarctic, Greenland and Tibet.

Preparation of the input-output data for global grid required a way to handle land and ocean pixels separately. As can be seen from Table 2, the MODIS data set contains 3 different sources of measurements of the AOD at 470, 550 and 660nm: “Corrected” values are derived from MODIS measurements over land ‘dark targets’ but do not provide data over bright arid regions, “Effective” values are derived from MODIS measurements over the ocean, and “Deep Blue” values are valid over bright surface pixels. As such it was necessary to combine “Corrected” and “Deep Blue” values to have the greatest coverage of land pixels. Where a value existed from both “Corrected” and “Deep Blue” sources, the mean was calculated. For ocean pixels, where a value existed from both “Effective” and “Deep Blue” sources, the mean was calculated. A mean was also calculated at coastline pixels where both a land and ocean value was available. Fig. 24 shows the global mean values of the AOD at 470nm obtained from the 3 MODIS derived measurement sources. The columnar water vapour (“H₂O”) distribution and the OMI AAOD at 500nm distribution are also presented.

We then proceeded to train a NN for each cluster in the 10-cluster partition of the global grid using daily synchronous MODIS H₂O and AOD(470, 550 and 660nm) inputs, co-located with AERONET Level 2.0 Version AVSD outputs applying the methodology described in Task C2 (see for example Fig. 19). In Phase C our NNs were validated against co-located AERONET data and at the daily, weekly and monthly timescales. Moving to the global grid makes this prohibitive. The reason for this is that while it is possible to perform a validation on a pixel to pixel basis, the global grid contains 64800 pixels (360 longitude x 180 latitude) and,

as shown in Fig. 7 the pixel occupancy of clusters in the thousands. This makes validation at different temporal scales across the grid prohibitive. We adopted a simpler approach based on setting aside 20% of the synchronous and co-located training data set and validating each cluster by comparing the mean NN-retrieved AVSD and the mean AERONET-retrieved AVSD obtained from all pixels. This is shown in Fig. 25 for the 10 NN's trained and validated for each cluster.

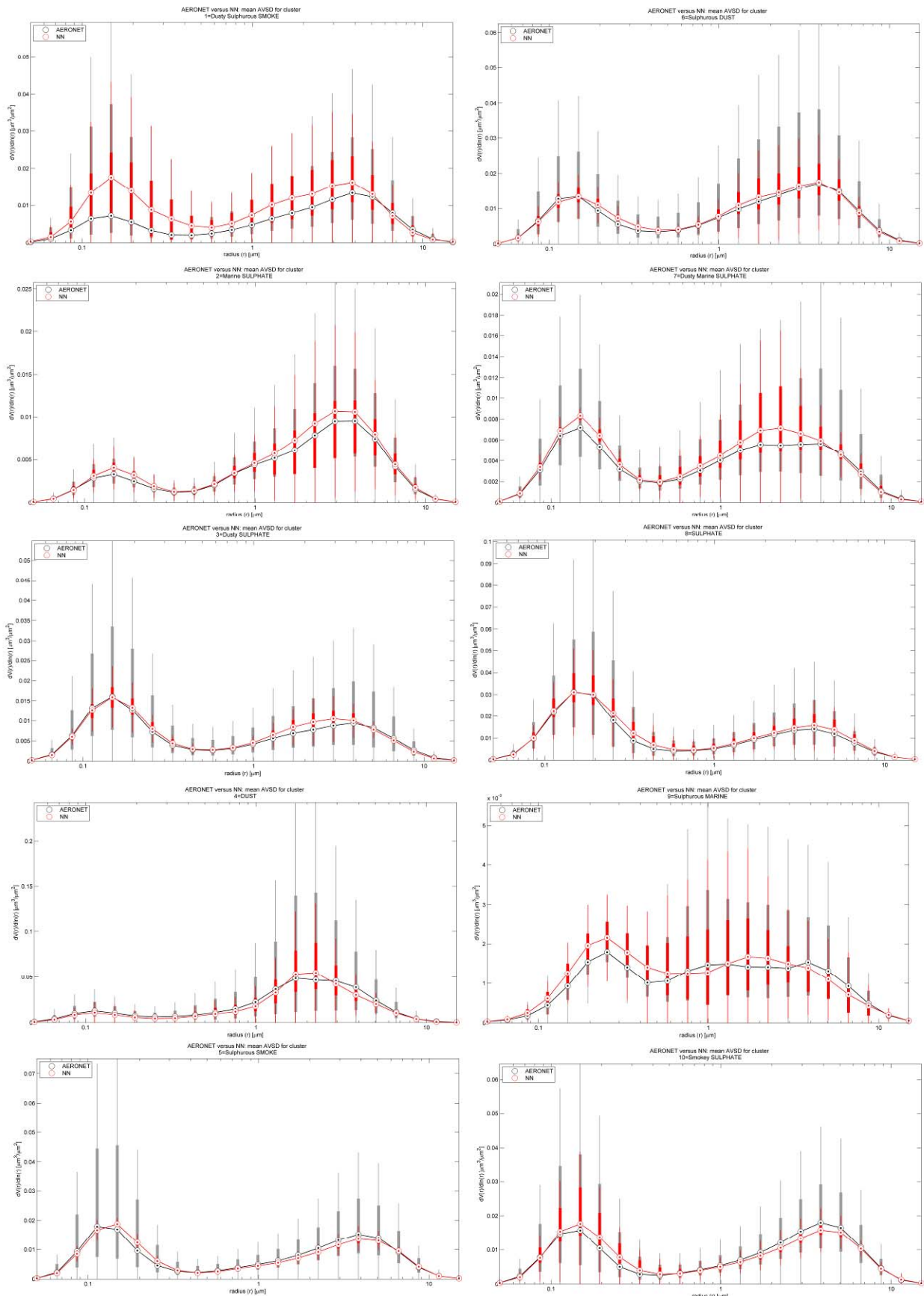


Fig. 25. The mean NN-retrieved AVSD (red) and the mean AERONET-retrieved AVSD (black) obtained for all pixels in each of the 10 clusters partitioning the global grid. In each of the 22 radial bins, the inter-quartile range (IQR) is shown as a bar and outliers are shown as thin lines extending out to the median $\pm 1.5 \times \text{IQR}$.

The 10 trained and validated NNs were then presented with homogeneous satellite inputs to generate global map. So, for example, homogeneous values of H₂O, AOD(470, 550 and 660) over each of the pixels of the global grid comprising the dust-dominated cluster 4 were fed as inputs to the trained and validated NN-4 and the 22-bin AVSD was retrieved for each pixel. Figs. 26-28 below show the seasonal mean values of the fine and coarse volume concentrations over land and the fine mode fraction:

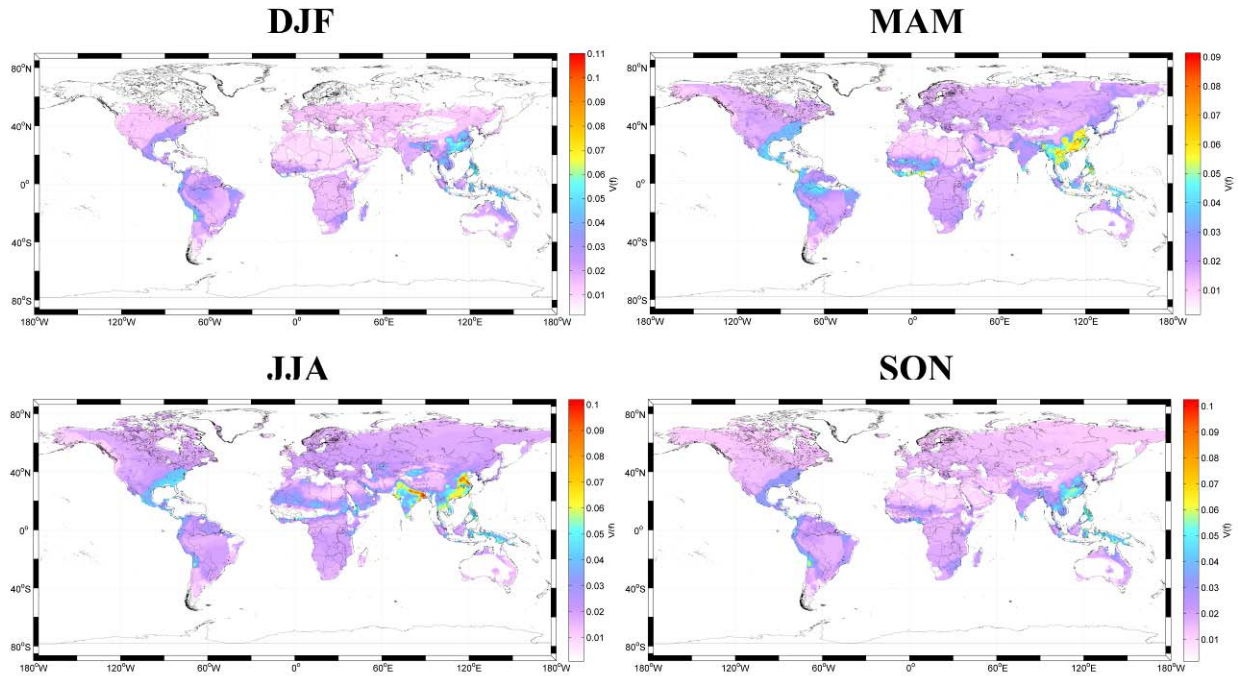


Fig. 26. Global seasonal maps of the volume concentration of the fine mode $V(f)$ from NN-retrieved AVSDs.

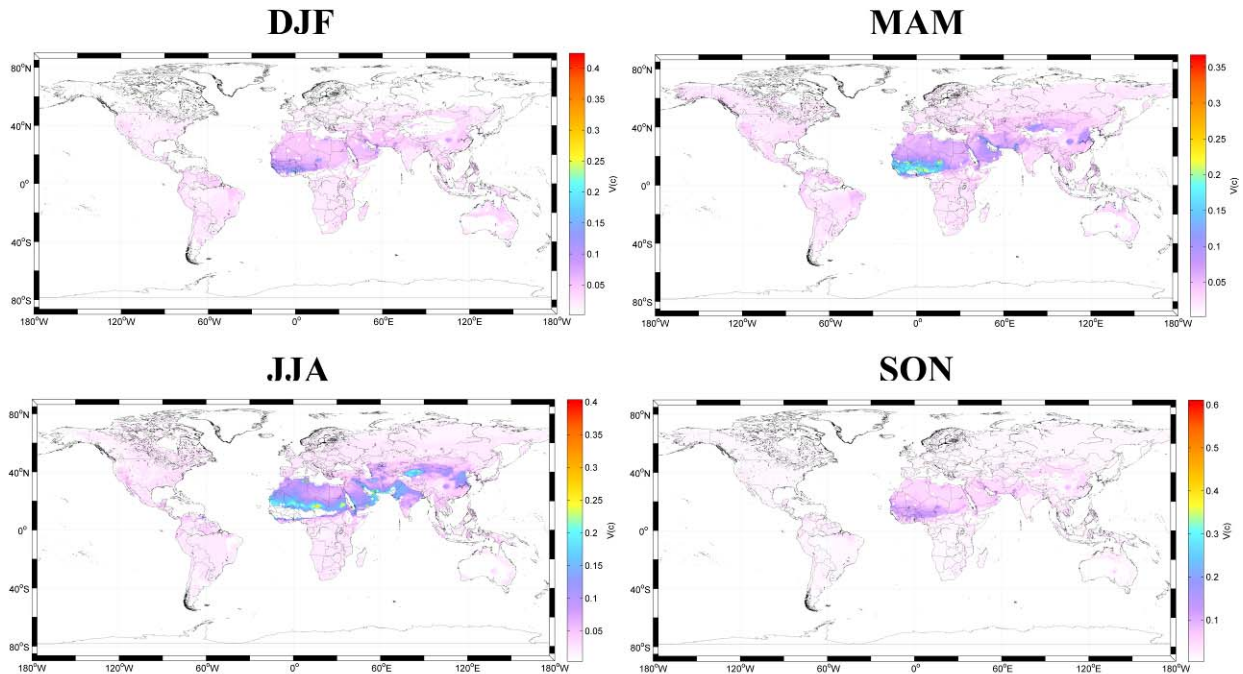


Fig. 27. Global seasonal maps of the volume concentration of the coarse mode $V(c)$ from NN-retrieved AVSDs.

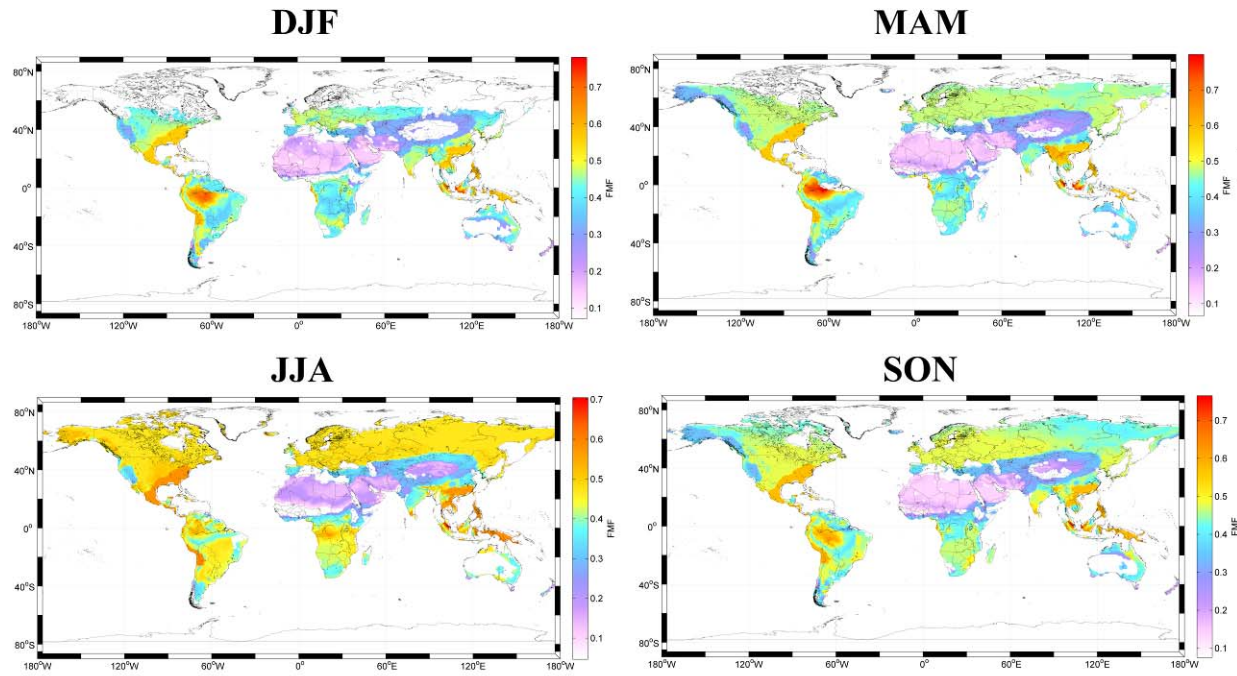


Fig. 28. Global seasonal maps of the fine mode fraction FMF from NN-retrieved AVSDs.

The 10-cluster partition of the global grid by aerosol type/mixture facilitated the construction and validation of NNs that are capable of rendering global maps of aerosol microphysics. This allowed us to achieve deliverable 7:

Deliverable 7: Rendering of global ANN-derived AMP maps with aerosol typing.

At the daily timescale a problem was faced. We realized that, although homogeneous satellite inputs are available on a daily basis, many pixels can be empty – especially when atmospheric conditions are not ideal for the acquisition of measurements (e.g. cloudy skies or low aerosol loads). This situation is illustrated in Fig. 29 below:

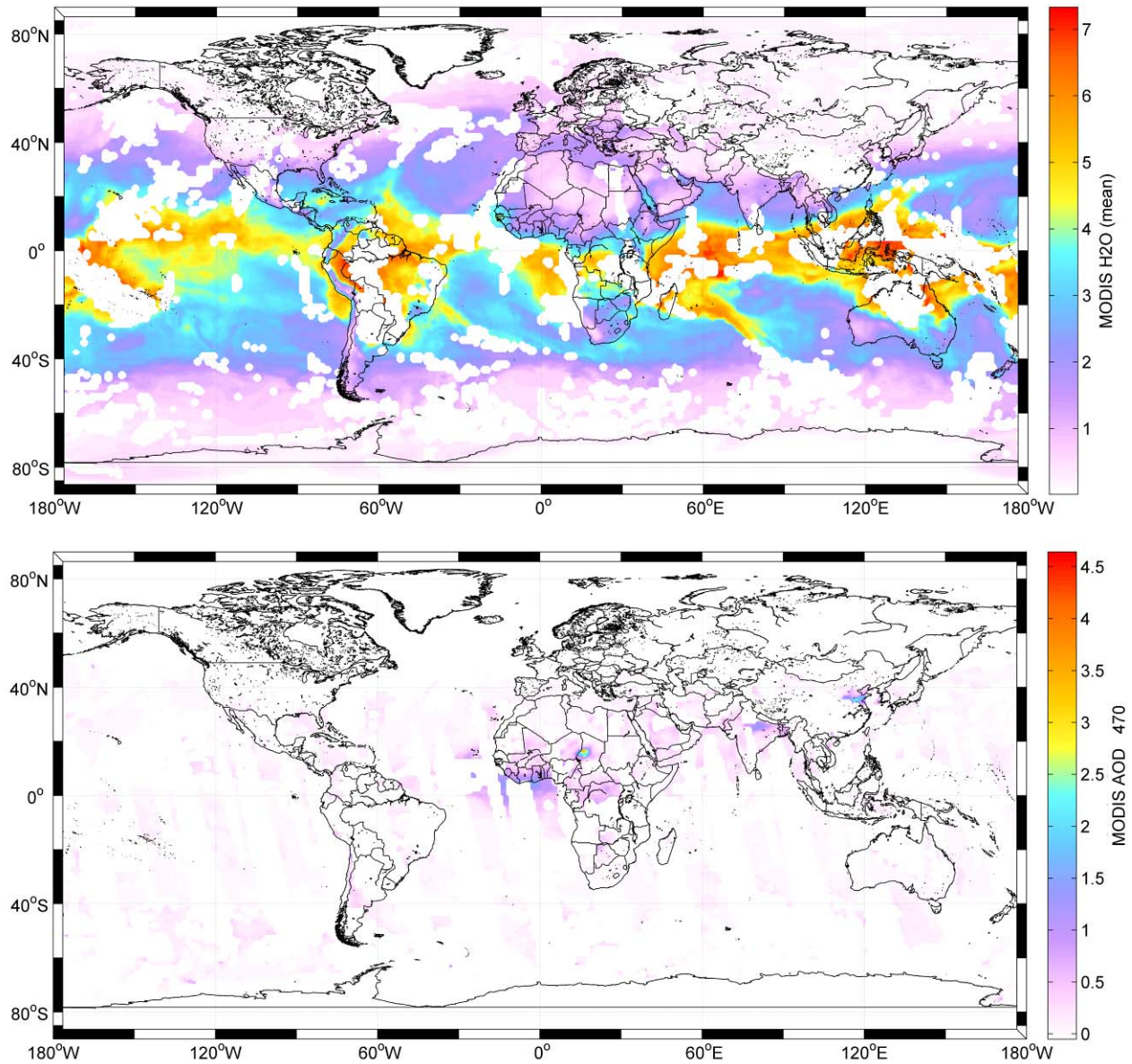


Fig. 29. Global satellite measurements of H₂O (top) and AOD at 470nm (bottom) on the 12th of January 2007.

The resulting daily global maps of Vf and FMF produced by feeding the 10-NNs with the satellite inputs of Fig. 29 at a resolution of 1x1 degree are shown in Fig. 30:

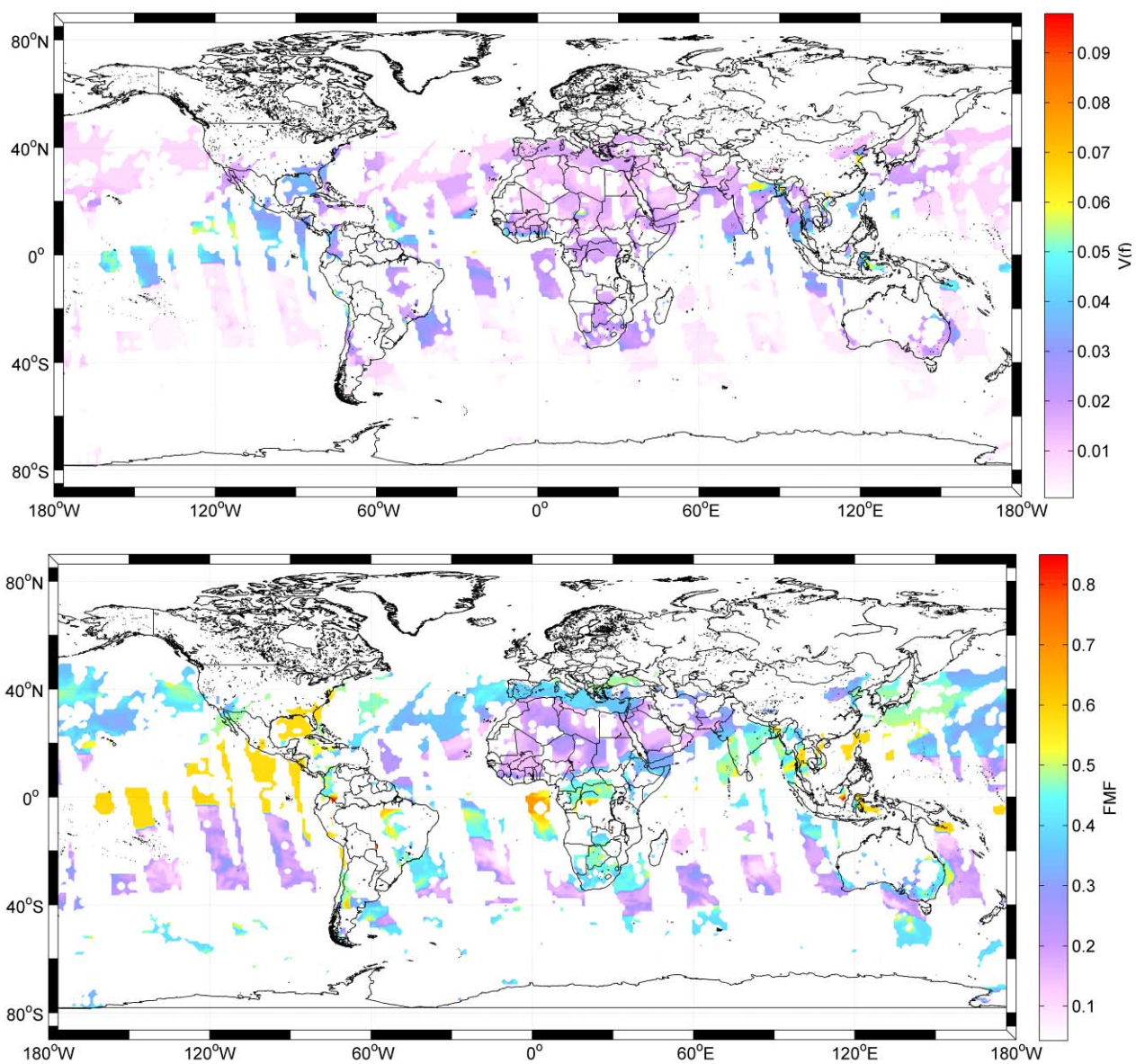


Fig. 30. Global retrieval of AMP parameters: Vf (top) and FMF (bottom) on the 12th of January 2007.

This demonstrated the ability of AEROMAP to produce daily-updatable, global maps of AMP on the global grid. Task C3 was completed in month 18 (3-months later than scheduled), satisfied Objective 7 and led to Deliverable 8:

Deliverable 8: Production of accurate, daily-updated, global maps of AMP on a global grid of resolution 1 degree CMG.

PHASE D: (months 18-24)

TASK D1 (months 18-21): Assessment of real-time monitoring

Task C3 revealed a problem with monitoring at the daily timescale – i.e. that global satellite inputs are patchy at this temporal scale. It was therefore decided to extend the temporal window in order to see at what scale an acceptable number of pixels provide input data for practical use. For this purpose, we identified an event to monitor that took place over a 2 week period – the eruption of the Madagascar

Karthala volcano between th 12th and 23rd of January 2007 whose evolution is shown in the GOCART reconstructed images in Fig. 31 below:

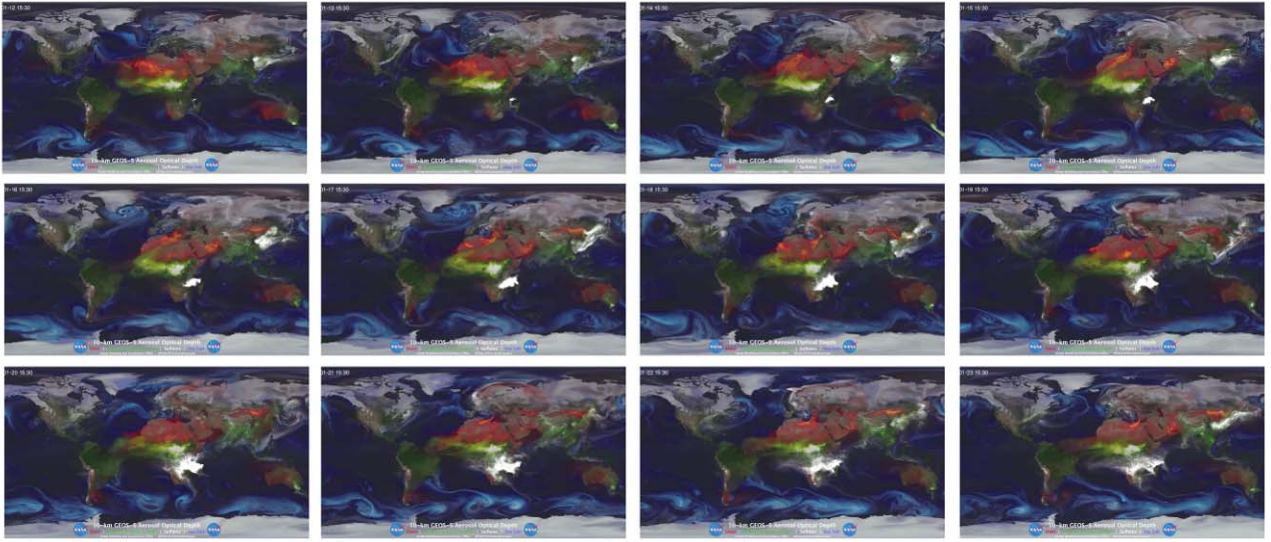


Fig. 31. Reconstructed global GOCART images of overlaid dust (red), biomass burning OC+BC (green), sea salt (blue) and sulphate (white) on 12 days spanning the temporal interval 12th to 23rd of January 2007 (date order is left to right and then top to bottom).

Fig. 31 shows a small white dot off the eastern coast of southern Africa at Madagascar which steadily grows in magnitude and extent. To test the feasibility of monitoring this event with AEROMAP we found that the best balance between retaining a high sampling rate and spatial coverage of homogeneous inputs was obtained with a 4-day window (i.e. by averaging pixel inputs over a 4-day period and then using the 10-NN model to calculate the AVSD in each pixel and extract microphysical parameters). At this temporal scale, Fig. 32 below compares the reconstructed 4-day GOCART image with the 4-day values of Vf calculated over land:

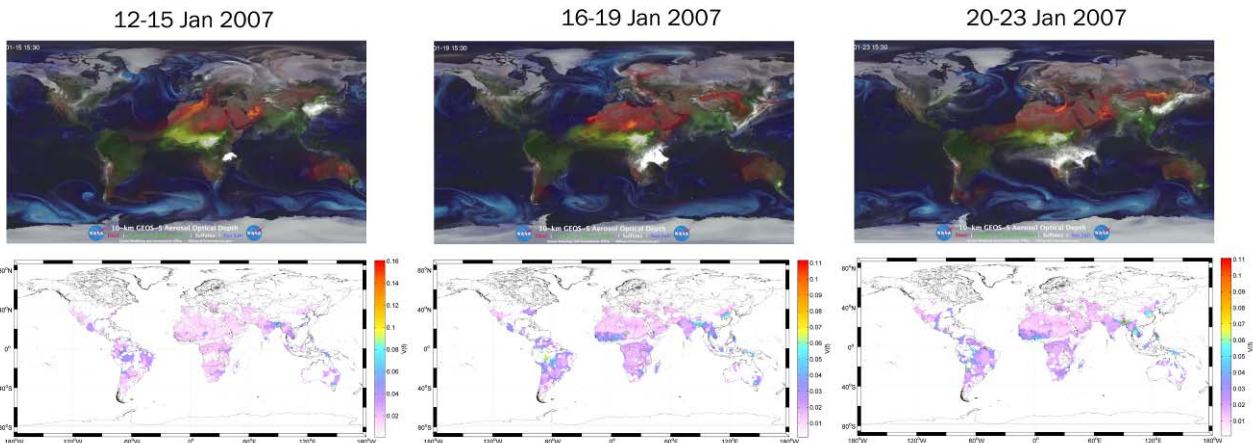


Fig. 32. Reconstructed 4-day global GOCART images of overlaid dust (red), biomass burning OC+BC (green), sea salt (blue) and sulphate (white) during the Karthala eruption (top panels) and the Vf derived from 4-day satellite inputs over land (bottom panels).

The 10-NN model Vf output corresponds well with some centres of high sulphate activity. However, clearly the spatio-temporal dispersion of sulphate from the Karthala eruption spans both land and ocean pixels. To investigate this more closely, the simulation was re-run for southern Africa below the equator using homogeneous 4-day averaged land and ocean satellite inputs fed to the NN model. Fig. 33 compares the regional 4-day GOCART reconstructed images with the 4-day retrieval of Vf obtained by our model:

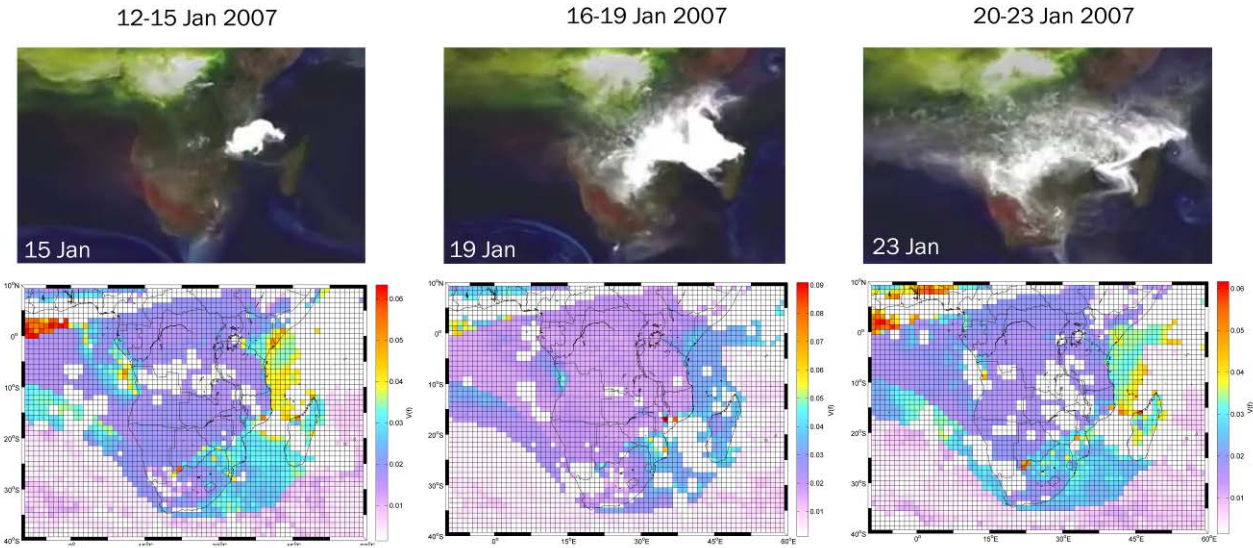


Fig. 33. Reconstructed regional 4-day global GOCART images of overlaid dust (red), biomass burning OC+BC (green), sea salt (blue) and sulphate (white) during the Karthala eruption (top panels) and the Vf derived from regional 4-day satellite inputs over land & ocean fed to our NN model (bottom panels).

Fig. 33 shows clearly the distribution of fine aerosol associated with the volcanic eruption and its spatio-temporal dispersion. The result is satisfactory. Although there is patchiness in the global provision of homogeneous satellite inputs, averaging on a timescale of 4-days means that the spatio-temporal dispersion of aerosol associated with events of this nature can be modelled with AEROMAP.

Task D1 was completed in month 21, satisfied Objective 8 and led to partial fulfilment of Deliverable 9:

Deliverable 9: A global real-time monitor of aerosols and alerting service for the assessment of climatological risks and the issuing of early-warnings

Our study of the 3D spatio-temporal dispersion of sulphate from the Karthala volcanic eruption showed that real-time monitoring at the daily timescale, while produced by the AEROMAP methodology, is not practical at this scale due to the patchiness of homogeneous satellite inputs. The study above demonstrated the feasibility however, of real-time monitoring on the 4-day timescale. Refer to Section 2.3.2 and Section 2.3.5 for more discussion on this slight deviation from the Work Plan and as assessment of its potential impact on project outcomes.

TASK: D2 (months 21-24): Implementation of the real-time monitor and alerting service

While Task D1 succeeded in demonstrating the feasibility of our methodology for near-realtime monitoring, implementation of a real-time monitor requires installation of a MODIS antenna to automatically obtain fully real-time daily data. This was not foreseen at the start of the project but the host institute is nevertheless in the process of acquiring and installing a MODIS antenna. This will provide the capability of the AEROMAP algorithm to perform real-time monitoring post-project completion. See Section 2.3.2 and Section 2.3.5 for more discussion on this small deviation from the expected results.

In order to develop an alerting service for the real-time monitor, Task D2 required that indices that measure the potential impact of aerosols be constructed. Various air quality indices (AQI) have been produced by national authorities to communicate to the public how polluted the air is currently or how polluted it is forecast to become. An AQI can go up (meaning worse air quality) due to a lack of dilution of air pollutants associated with stagnant air caused by anticyclones, temperature inversions, or low wind

speeds. Different countries have their own air quality indices which are not all consistent. To present the air quality situation in European cities in a comparable and easily understandable way, all detailed measurements are transformed into a single relative figure: the Common Air Quality Index (or CAQI). The CAQI has 5 levels using the following scale: 0-25 (very low), 25-50 (low), 50-75 (moderate), 75-100 (high) and > 100 (very high) and is a relative measure of the amount of air pollution. It is currently based on 3 pollutants of major concern in Europe: PM10, NO₂, O₃ and will be able to take into account to 3 additional pollutants (CO, PM2.5 and SO₂) in coming years. As such it is based on chemical data from city-based stations or road-side monitors.

Since air quality is defined as a measure of the condition of air relative to the requirements of one or more biotic species or to any human need or purpose, we decided to construct 2 indices: an AQI to measure the potential impact on health and an AQI to measure the potential impact on visibility (but not necessarily on health). Traditionally, to compute the AQI requires an air pollutant concentration from a monitor or model. As with the CAQI, the function used to convert air pollutant concentrations to AQI varies by pollutant. AEROMAP calculates the AVSD and its secondary microphysical parameters in each pixel of the global grid at the daily timescale. While it does not directly measure the chemical composition of the atmospheric column, the volume concentration of fine mode (V_f) and coarse mode (V_c) particles provide quantitative measures of the amount of small and large particles in the atmosphere. AQI values are typically divided into ranges where each range is assigned a categorical code and a standardized public health advice message. While there is no internationally-agreed standard for AQI scales and directives yet, in line with our deliverable of creating such an index, we constructed a normalized scale from 1-10 derived from 5 categories common to many of the existing AQIs. To achieve this, we first calculated 4 break-points based on quantile values of V_f and V_c as shown in Fig. 34 below:

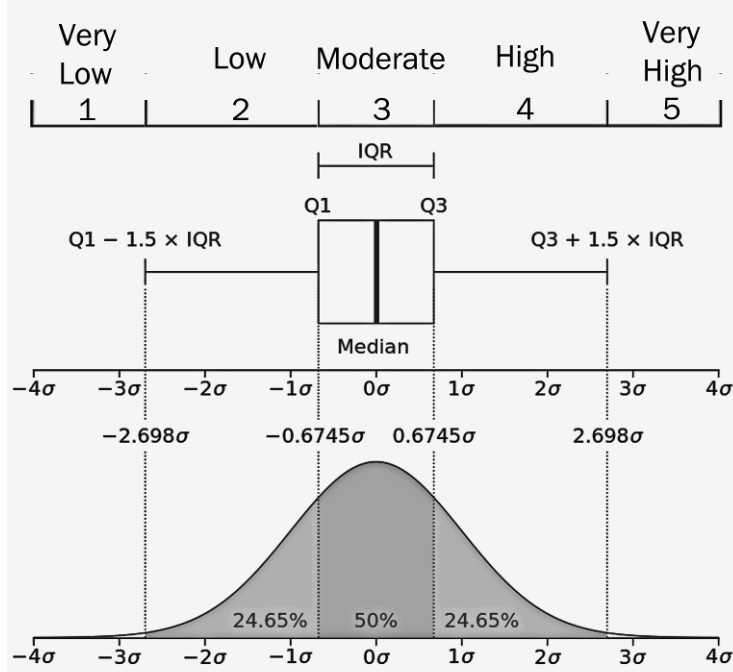


Fig. 34. From the global distribution of values of the fine and coarse particle volume concentrations (V_f and V_c respectively), 4 break-points at Q1-1.5IQR, Q1, Q3 and Q3+1.5IQR were calculated and used to assign the V_f and V_c in each pixel with one of the 5 categorical AQI bands (1-5).

The AQI of impact on health (which we call “AQI (health)”) in each pixel was then calculated from a simple linear weighted sum (a ratio of 9:1 gave best results) of band(f) (i.e. the band in which V_f falls) and band(c) (i.e. the band in which V_c falls):

$$\text{AQI (health)} = [9 \times \text{band}(f) + 1 \times \text{band}(c)] / 5$$

The factor of 5 in the denominator is required to normalize this AQI scale to the range 1-10 (e.g. assuming that Vf is at its peak with band(f)=5 and Vc is also at its peak with band(c)=5, then $AQI = 9 \times 5 + 1 \times 5 = 50$ and a division by 5 is required to scale this to a maximum value of 10). Similarly, the AQI of impact on visibility (which we call “AQI (visibility)”) in each pixel was then calculated from the linear weighted sum (a ratio of 1:3 gave best results):

$$AQI (\text{visibility}) = [1 \times \text{band}(f) + 3 \times \text{band}(c)] / 2$$

Fig. 35 below shows the values of AQI(health) and AQI(visibility) calculated from the value of Vf and Vc in each pixel resulting from the AVSD output from feeding NNs with mean satellite inputs over the period 01/10/2004 to 16/04/2012:

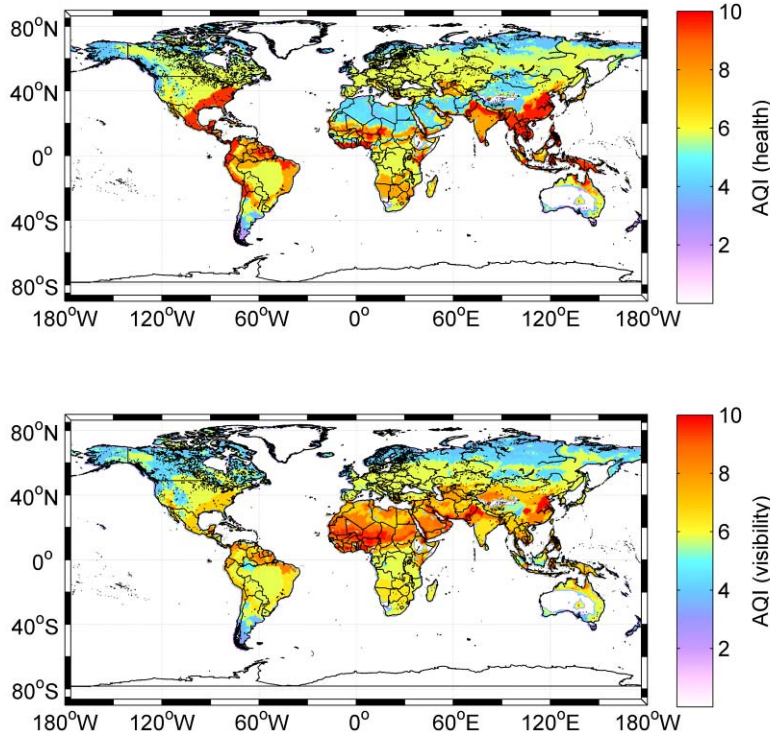


Fig. 35. The global mean values of AQI(health) and AQI(visibility) on the normalized scale 1-10.

Fig. 35 seems to be consistent with our present understanding of aerosols, i.e. that very high AQI(health) values are seen in the US east coast, south-east Asia, megacities in south America, and the north of Indian sub-continent where urban pollution is high. This is also the case for cities at the periphery of biomass burning regions. Biomass burning regions themselves present moderate to high mean values (also seen in India and the north of Australia). Europe and the central-west of the USA has moderate AQI(health values) and western Canada, northern Russia, the dust belt and Tibet have low values. The lowest land-based AQI(health) values are seen in the south of Chile and Patagonia and in western Australia. With respect to AQI(visibility) which is associated with large (mainly dust and sea spray) aerosol, the most affected regions having very high values are the Sahel, the northern coast of Africa, the Arabian peninsula and Kashmir. The region around Beijing is also strongly affected presumably by the influx of dust from Gobi desert. Moderate to high values are observable in biomass burning regions due to smoke, the eastern coast of the US and large parts of Europe due to urban smog. Low values of AQI(visibility) are observed in western Canada, northern Russia (and parts of Europe) and in southern Argentina. The lowest values are again seen in western Australia. Following completion of the project, the fellow will be employed at the host institute and will continue to work on improving satellite-based and microphysics-derived AQIs. In particular, he will

validate them against co-located and synchronous AQIs derived from ground-based chemical measurements and models.

As described in Task D2, the host institute is about to install a MODIS antenna which will allow for automatically obtaining satellite measurements which can be fed to the NNs produced by AEROMAP and used to simulate daily aerosol microphysics. In preparation for the issuing of alerts once the real-time monitor comes online, the following public alerts have been drafted based on the normalized values of AQI(health) and AQI(visibility) described above:

AQI band	Value	Health message	Visibility message
Very Low	1–2	Enjoy your usual outdoor activities.	No impact.
Low	3–4	Members of the public with lung or heart problems should <u>consider reducing</u> strenuous physical exertion, particularly outdoors.	Transport authorities should <u>consider monitoring</u> aerosol forecasts.
Moderate	5–6	Members of the public with lung or heart problems should <u>reduce</u> strenuous physical exertion, particularly outdoors.	The public should <u>reduce</u> unnecessary transport.
High	7–8	All members of the public should <u>avoid</u> strenuous physical activity outdoors.	The public should <u>avoid</u> transport as the risk of accident is high.
Very High	9–10	Members of the public with lung or heart problems <u>are at risk</u> .	Members of the public being transported <u>are at risk</u> .

Task D2 was completed in month 24. AEROMAP has produced and tested an algorithm for real-time monitoring and has constructed AQIs and alerts needed for satisfaction of Objective 8 and Deliverable 9:

Deliverable 10: A global real-time monitor of aerosols and alerting service for the assessment of climatological risks and the issuing of early-warnings.

Bi-Product: A new line of research has been initiated to globally-validate the satellite-derived microphysics-based AQIs against chemical-based AQIs.

PHASE E: (Months 1-24)

TASK E2 (months 12-24): Public engagement about the project and the role of Marie-Curie Actions and atmospheric chemistry

During Task E1, the fellow designed and produced the project website which can be found at the location: <http://apcg.space.noa.gr/aeromap>. In the second 12 months of the project, substantial new content was continuously added to the project website in order to engage the public on its progress and on the role of Marie-Curie Actions and on the subject of atmospheric chemistry. In particular, the website now:

1. provides a non-technical description of climate change and the role of the global aerosol system with links to non-technical resources and multimedia
2. provides a non-technical description of the project
3. describes in detail the project participants, co-authors and has prominent links to the host institute
4. provides transparency by allowing public access to the project proposal description
5. shows the full progress of the project on a timeline of the work plan and indicates project objectives, milestones and results delivered
6. provides open access to the dissemination of results in peer-reviewed publications, conference proceedings, posters and graphics produced during the course of the project
7. provides contact details for submission of public queries on the project that will be answered by email

8. contains an education gateway complete with links to video animations, approachable feature articles in the popular science press, and lecture courses as part of the Open Course Ware initiative
9. contains global data outputs (including global maps of AQIs) produced by AEROMAP.

A Twitter account (<https://twitter.com/AEROMAP>) has been used to announce publications and has resulted in a lot of traffic and high alt-metrics (PDF downloads and HTML views) at the online open access articles published. The two researcher and education gateways added to the project website have facilitated interaction with non-specialist visitors and educationists, providing them with informative content. Please see Section 2.3.6 for further information on the development of the project website.

TASK E3 (months 12-24): Outreach mass media activities

During this period, the fellow paid significant attention to dissemination of results in the form of peer-reviewed articles and conference papers so as to engage as large an audience as possible. The important role played by Marie-Curie Actions in facilitating the work has been acknowledged on each publication to make clear and prominent the role of the project in European research and enabling mobility, and the work currently being funded and undertaken in the ERA on the global aerosol system. The success of this programme of science communication activities led to satisfaction of Objective 9. On project completion, the fellow will write a formal press release to communicate the main findings of the project. This press release will be sent to national scientific bodies, newspaper broadsheets with science sections, EC news outlets and to popular science magazines.

TASK E4 (month 24): Public talk

On the 9th of April the fellow will give a public talk describing the project, the role of Marie-Curie Actions in supporting mobility and the relevance and importance of the findings for advancing our understanding of global aerosols and our ability to globally monitor aerosol pollution and its impact on climate change. The Power-point version of the talk will be made available on the “Media” section of the project website.

2.3 Project management during the period

2.3.1 Management tasks and achievements

The host institute and in particular the SIC, has successfully provided research supervision, expertise and has facilitated collaborations essential for the advanced training needs of the fellow. Following provision of a comfortable workspace in the ACP Group at IERSD-NOA and incorporation of the fellow into the group and its website, the SIC helped the fellow smoothly through the process of registering with the Greek tax office, obtaining health insurance, arranging payment and generally settling in to his new environment. Necessary technical equipment (namely the purchase of a state-of-the-art desktop PC for the project) and software (namely MATLAB) was made an immediate priority and quickly acquired. On the technical side, the SIC assisted the fellow in accessing and obtaining satellite remote sensing and ground-based datasets and showed his great experience in this regard – allowing the fellow to get up to speed rapidly. As a result, the first neural networks were trained within the first 4 months of the start date and gave the fellow the opportunity to meet the call for abstracts at the European Aerosol Conference 2012 where the first results of the project were presented. In addition, the SIC early on capitalised on his collaboration network and opened up a collaboration with the University of Ioannina where Dr Antonios Gkikas had recently developed a more precise technique for sampling MODIS pixel data. Furthermore, the SIC placed the fellow in contact with an expert on airborne aerosol measurement and retrieval, Dr Alexandra Tsekeri, who has recently completed her doctorate at the City University of New York. In particular, Dr Tsekeri’s experience of handling measurement errors has helped arm the fellow with the knowledge base needed for developing precise neural network results from satellite data whose uncertainties can be quantified. The SIC has also taken steps to ensure that the algorithms, computational tools and data to be developed and acquired during this project will be made available at the project website/portal and incorporated into the Greek GEO Office data centre. Technologies developed by AEROMAP will also be included in the National Bank of Environmental Observation which is coordinated by NOA. In particular, the Greek GEO Office which since

2008, has initiated an inventory of meteorological and atmospheric data coming from the Public Sector, Research Institutes and Universities, ensures that its national portal harmonizes and shares data among producers, providers and policy-makers in the field of environmental observation. This database will be enhanced with the climatological data collected during the operation of AEROMAP which is expected to assist the identification of gaps between available and required Earth observations. AEROMAP's databases will be linked to existing Earth Observation portals and online resources and the portal will enable users to access and download data, products, algorithms and tools. The invitation of the fellow to be part of NOA and to lead the project is bringing international expertise and interdisciplinary research to the host institute and helped raise the profile of the fellow. Finally, the host institute's ground-based Atmospheric Remote Sensing Station (ARSS) is the federated site of AERONET that monitors aerosol pollution over the city of Athens. As a result, the fellow as a member of the ACP Group is in direct contact with scientists that are expert in aerosol measurement, online data provision and database management. This skill base has proved invaluable as the project progressed into Phase D and the development of the algorithm for global real-time monitoring. The fellow has also been provided with access to UV radiative-transfer codes and to the European UV database should the need arise and time permit the assessment of atmospheric radiative-budgets. In summary, the general scientific arrangements required for the success of this project have been comprehensively provided to the fellow including: a) access to satellite aerosol databases, b) access to ground-based aerosol retrievals and techniques, c) access to a high-tech AERONET station, d) access to PCs, computing power, resources and software for the coding and running of neural networks, and image processing and web development software, and importantly, e) access to expertise in the field via direct interaction with or via the collaborative networks connected with APC group members. The wealth of experience that the host institute has in accommodating visiting scientists and implementing projects of this scale, has meant that AEROMAP has progressed smoothly and could deal with new challenges smoothly. The regular personal mentoring by the SIC and regular group meetings have enabled the fellow to flourish.

TASK: To help the fellow acquire competencies in the field of environmental modelling

The expert training provided to the fellow by the SIC during frequent (weekly) project meetings has meant that a steep learning curve was achieved quickly in this rapidly developing research area. The fellow now has a high level of technical background knowledge in the field of global aerosol characterization and measurement. This is evidenced by the publication of 4 peer-reviewed publications in top atmospheric physics journals and acceptance of 2 conference papers in the proceedings of the prestigious International Conference on Meteorology, Climatology and Atmospheric Physics. Furthermore, an additional 3 manuscripts are at submission stage – strongly enhancing the fellow's publication record and contributing to increased visibility and impact of his research. The very positive climate of collaboration engendered at the host institute has allowed the fellow to be well integrated in the ACP Group. An early outcome of this has been the introduction of the fellow to the wider environmental research, remote sensing and atmospheric chemistry and physics community. The fellow is acquiring strong competencies that are establishing him as an independent scientist in the field of satellite retrievals and aerosol modelling. These achievements of the project are testament to the successful collaboration between the fellow and the SIC and the transfer of knowledge of between their corresponding fields of expertise: applied mathematics and environmental research. The high volume of traffic that the pages of the project website are attracting, combined with a growing social media presence on Twitter are giving added weight to the national and European presence of the fellow in a rapidly evolving field, and are helping in the formation of new collaborations between the fellow, the host institute and other foreign research groups in the field of environmental research. Finally, the scientific experience of the SIC and the host institute have ensured the effective exploitation of the results of the project.

TASK: To contribute to the career development and re-establishment of the fellow

One of the principal goals of the fellowship in terms of the medium to long-term development of the fellow's career is to enable the fellow to achieve the level of principal investigator as a medium term goal,

and to help him secure a permanent research or academic position in the field of environmental modelling in atmospheric physics as a long-term goal. The project funding from a Marie Curie IEF has provided the mobility that enabled the fellow to relocate at an expert host institute where he has been able to interact and collaborate with world-leading researchers in the field. As a result, he has obtained competence in the fields of aerosol science, remote sensing, measurement techniques, atmospheric physics and chemistry modeling. As such, the fellowship has supported his transition from an applied mathematician applying advanced methods in several academic disciplines, to an experienced scientist in the field of environmental research. The fellowship, in addition to helping focus the fellow's skills in one field, is also supporting the fellow's transition to research independence. The fellow has already taken a leading role in terms of the implementation of project work plan and the development of the AEROMAP website. The close collaboration between the fellow and the SIC has led to significant new results and numerous peer-reviewed research publications that have strengthened the fellow's CV. Furthermore, the fellow has developed the skills required to manage a project of this scale and importance - which will be a valuable asset in the future when he applies for more senior scientific positions. Working at the host institute has exposed the fellow to the operational algorithms of satellite-based instruments, to global monitoring and mapping techniques and to ground-based atmospheric information analysis. His involvement with the latest methodologies used to obtain aerosol retrievals from the satellites MODIS and OMI, the global chemical model GOCART, and the ground-based AERONET stations has provided him with in-depth knowledge of contemporary measurement techniques, retrieval methodologies, uncertainties and limitations associated with remote sensing of aerosols from space and ground. Furthermore, the techniques he has developed and has applied are supporting the call of the IPCC to greatly expand efforts to monitor and globally-characterize aerosols. The successful completion of the project has substantially enriched the fellow's research profile and is helping him establish a professional career in the field.

TASK: To contribute to European excellence and competitiveness

AEROMAP is contributing to one of the most important climate change parameters – the global distribution and composition of atmospheric aerosol. As such, the project is helping to raise the profile of the ERA for researchers in this field. The large number of published results have contributed to European excellence and competitiveness by demonstrating that European centres like the host institute NOA are pioneering new methods to exploit satellite remote sensing and are making a major contribution to efforts to globally-monitor and characterize aerosols. Furthermore, the use of cutting edge mathematical/computational methods like neural networks, cluster analysis, Gaussian mixture models and state-of-the-art mapping techniques, implemented in AEROMAP contribute to the creation of a pole of attraction for scientists from outside the ERA who will be interested in learning such techniques, applying them in their own fields of research, or incorporating them in existing operational aerosol retrieval algorithms. The cross-fertilisation of knowledge that this engenders is helping raise the status of European science as originator of such methodologies and will hopefully attract more talent to the ERA. The project website has matured into a showcase for the project, the fellow, the host institute and Marie Curie actions in general. It now houses global maps of aerosol microphysical properties and characteristics not provided anywhere else. The real-time monitoring algorithm, aerosol impact index and aerosol hazard alerts developed are highly innovative products and will hopefully attract a wide audience. The research findings produced by AEROMAP have the potential to help reduce the uncertainty associated with the impact of aerosols on the planetary radiation budget, and this in turn is expected to have a positive impact on environmental policy-making decisions worldwide – further drawing attention to the ERA as instigator. Until now, it has not been possible to exploit the full-Earth coverage provided by satellite remote sensing in order to globally-characterise aerosols via their microphysical properties. As a result Europe has followed the example of other continents in building instruments and investing in ground stations federated to AERONET. The methodology developed by AEROMAP for extrapolating AERONET retrievals from stations to off-site locations via the use of satellite inputs fed to neural networks, has been validated and is moderately accurate for deducing key aerosol parameters on the daily timescale. Small scale but high impact projects like AEROMAP are helping to ensure that Europe can meet the challenges of the 21st century where the quality of the environment

affects everyday life and the impact of aerosols on climate change, air quality and business (e.g. aviation) is high in the public conscience. Europe is strongly affected by inflows of dust from the Sahara and the Arabian Peninsula, biomass burning from wildfires like those in Moldova, Northern Greece, Spain and the coastline region of Portugal. One direct and long-term structuring effect of AEROMAP is that its products will allow for determination of the best sites to locate new AERONET stations to monitor such phenomena more accurately. This motivated choice of pilot studies performed by the fellow in his paper on multiple-mode aerosol identification via the size distribution.

2.3.2 Problems that have occurred and how they were solved or solutions envisioned

This ambitious project has encountered a couple of theoretical obstacles which have all been overcome. Early results at the end of Phase A revealed that the proposed use of only 3 MODIS satellite AOD measurements as inputs to the NNs was capable only of retrieving mean values of optical and microphysical parameters and not the daily trends in these parameters needed to attain the goal of real-time monitoring. This problem was solved by expanding the set of satellite inputs to include other parameters and then identifying which combination of available inputs is required for retrieving the daily variation of aerosol parameters. In particular, in the context of desert dust over an extensive region (Northern Africa), it was found that the columnar measurement of water vapour content from MODIS was required to supplement the 3 MODIS satellite AOD measurements as inputs in order to successfully retrieve the AVSD. This study was carefully focused, well founded and brought dividends including a publication in the *Journal of Atmospheric Measurement Techniques Discussions* describing this new approach. In order to check that this success was not confined to the case of dust, NNs using satellite inputs were also trained and tested during Phase B on co-located and synchronous satellite and AERONET data for biomass burning aerosol over an extensive region of the Amazon, and for urban sulphate aerosol in 2 northern hemisphere cities having a long data record (Washington-GSFC and Moscow-MSMU). As described in detail in the mid-term report for reporting period 1, the NNs were shown to be able to retrieve the required aerosol parameters to a satisfactory level of accuracy at the daily timescale required for the development of a real-time monitoring algorithm.

During Task C1, a serious technical constraint inherent to AERONET inversion products presented itself (see Section 2.1 for details). This meant that the proposed approach of applying cluster analysis to AERONET inversion products for distinguishing sites by aerosol type/mixture in Gobbi coordinates could not be adopted. To mitigate this, with the approval of the SIC, the fellow investigated other potential approaches for performing global aerosol typing and after some initial tests a methodology was developed based on downscaling mean global data from the GOCART chemical model to a 1x1 degree (latitude x longitude) grid (the same spatial resolution as the satellite products used as NN inputs) and then applying cluster analysis to the aerosol components (see Section 2.1 for details). This new methodology was able to achieve the required partitioning of the globe into distinct aerosol types/mixture regions. A secondary effect of this was that Deliverable 5 was modified slightly (see Section 2.1 for details). In parallel with this, during Phase C (months 9-15) the fellow was heavily involved in the co-authoring of 4 peer-reviewed articles which meant that, while Tasks C1 and C2 were completed successfully and bore additional fruit in the form of publications, an unforeseen delay of 3 months of research time was created. Task C3 was completed without a problem and Phase C of the project concluded in month 18 rather than month 15.

In Phase D, the fellow coded, trained and validated 10 NNs, one for each distinct aerosol type/mixture identified with the results of the cluster analysis developed in Task C1. This was an enormous challenge and involved isolating and data-processing co-located and synchronous satellite inputs and AERONET outputs in the 64800 pixels (360 longitude x 180 latitude) of the global grid. The first global maps of aerosol microphysical parameters were successfully produced in month 21 and a positive assessment was made regarding the potential of the NN-based algorithm to perform near real-time monitoring. This was verified also by a study of the 3D spatio-temporal dispersion of sulphate over Madagascar resulting from eruption of the Karthala volcano. However, the study showed that, while the AEROMAP algorithm successfully produces maps of AMPs, patchiness in the availability of satellite inputs on the daily timescale limited their

applicability on this temporal scale. Averaging over a 4-day timescale solved this problem and led to successful completion of Task D1. At this stage, it was realized that fully real-time monitoring will require the installation of a MODIS antenna at the host institute NOA to directly obtain data from the satellite instrument as it passes overhead. While this prevented immediate implementation of a real-time monitor, it is soon to be acquired and the AEROMAP algorithm will then, post-project, be able to start producing daily outputs in real-time. In preparation for this, the project also constructed multi-parametric indices of aerosol impact together with alerts (see Section 2.1 for details). The fellow has been contracted for 12 months by the host institute to continue evolving the AQIs and to validate them against those being produced from ground-based chemical measures.

The technical and theoretical problems described above and the mitigating actions taken to overcome them had a small negative effect on the projected work plan timeline – causing a delay of just over 3 months. On the one hand, the actions implemented led to a large number of (7) peer-reviewed publications which are greatly increasing the visibility of the project in the fields of aerosol science, remote sensing, atmospheric physics and measurement techniques. However, on the other hand, the need to focus more attention on the scientific component of the project was at the partial expense of some of the public engagement initiatives. In a project meeting between the fellow and SIC, a decision was made to mitigate this by engaging the public via exploitation of the project's growing online presence and the development of the Education Gateway at the AEROMAP website. Having presented an overview of the project at the European Science Open Forum in Dublin, Ireland in 2012 in the form of a manned digital poster session, and also at public seminars at the host institute, it was decided that the proposed public talk on Marie-Curie Actions and atmospheric chemistry (Task E2) could achieve the same goal by efficiently engaging the community via an Education Gateway where background information on climate change could also be housed. This decision helped raise the footfall at the project website and freed to the fellow to focus his efforts on the production of the algorithm and related tools needed for achieving real-time maps of aerosol parameters, and to focus on the preparation and revision of the large number of peer-reviewed publications produced during the second reporting period. The public talk of Task E4 (scheduled for month 23) will now take place post-project on the 9th of April at the Host Institute.

2.3.3 List of key project meetings, dates and venues

- Euro-Science Open Forum 2012, Dublin, Ireland: 11-15/07/2012
- European Aerosol Conference 2012, Granada Spain: 2-7/09/2012
- APC Group Seminar, NOA, Athens: 26/09/2012
- *Researchers Night 2012* at the National Hellenic Research Foundation, Athens: 28/09/2012
- APC Group Seminar, NOA, Athens: 01/04/2013
- CERN OA18 Workshop "Innovations in Scholarly Communication", Geneva, Switzerland: 19-21 June 2013.
- APC Group Seminar, NOA, Athens: 24/09/2013
- Public talk at NOA, Athens: 09/04/2014
- 12th International Conference on Meteorology, Climatology and Atmospheric Physics, Heraklion, Crete: 28-31/05/2014.

2.3.4 Project planning and status

A project meeting has been held on a weekly basis between the research fellow and the scientist in charge. These meetings have proven invaluable in that:

1. they allowed communication to the SIC from the fellow of the progress of the work
2. they allowed the fellow to learn from the expertise of SIC
3. they functioned as efficient brainstorming sessions for new ideas to advance the work

4. they allowed solutions to be found to mitigate unforeseen problems as they arose
5. they allowed the SIC to help the fellow in managing the workload efficiently
6. they allowed the SIC to assist the fellow with administrative paperwork related to routine administrative matters.

The project has progressed smoothly and, in addition to achieving the stated project deliverables, they have enabled the efficient production of additional bi-products.

2.3.5 Impact of possible deviations from the planned milestones and deliverables

As described in Section 2.3.2, Deliverable 5 was slightly modified (global maps in Gobbi coordinates were found to be both unsuitable and not necessary). Deliverable 9 was partially-achieved in that an algorithm capable of producing global maps of AMPs from daily satellite inputs was developed and tested, fully real-time monitoring was not able to be implemented due to the absence of a MODIS antenna. All other stated project deliverables have been fully met including the development of new AQIs and associated health and visibility alerts. Technical obstacles encountered during the course of the project were overcome and solutions were found to mitigate problems that arose in all cases. All 4 of the stated milestones were also achieved. Indeed, as this report hopes to show, many additional bi-products have been created as a result of novel problem-solving strategies introduced, and from the new collaborations the fellow is building with the worldwide environmental modelling community facilitated by the host institute. Finally, while the additional time involved in co-authoring the large number of peer-reviewed publications produced by the project was not factored into the proposed project timeline, this investment brought dividends in terms of engaging and generating interest within the scientific community. While this was at the expense of time originally allocated to engaging also the public, it is hoped that the science communication elements incorporated into the Education Gateway, the press release to be published on project completion, and the public talk next month – will help to mitigate this. The contracting of the fellow at the host institute to fully implement the real-time monitor and to evolve and validate the AQIs will mean that the project will have continued impact post-completion. It is envisaged that the real-time monitoring algorithm produced, the AQIs and alerts and the novel global maps of aerosol microphysics will have a substantial impact on policy-making decisions and the public understanding of the impact of aerosols worldwide.

2.3.6 Development of the Project website

As a result of completing Task E1, an extensive project website was designed and produced, housed at the host institute's website: <http://apcg.space.noa.gr/aeromap>. The website was further developed during tasks E2 and E3. The home page is shown below:

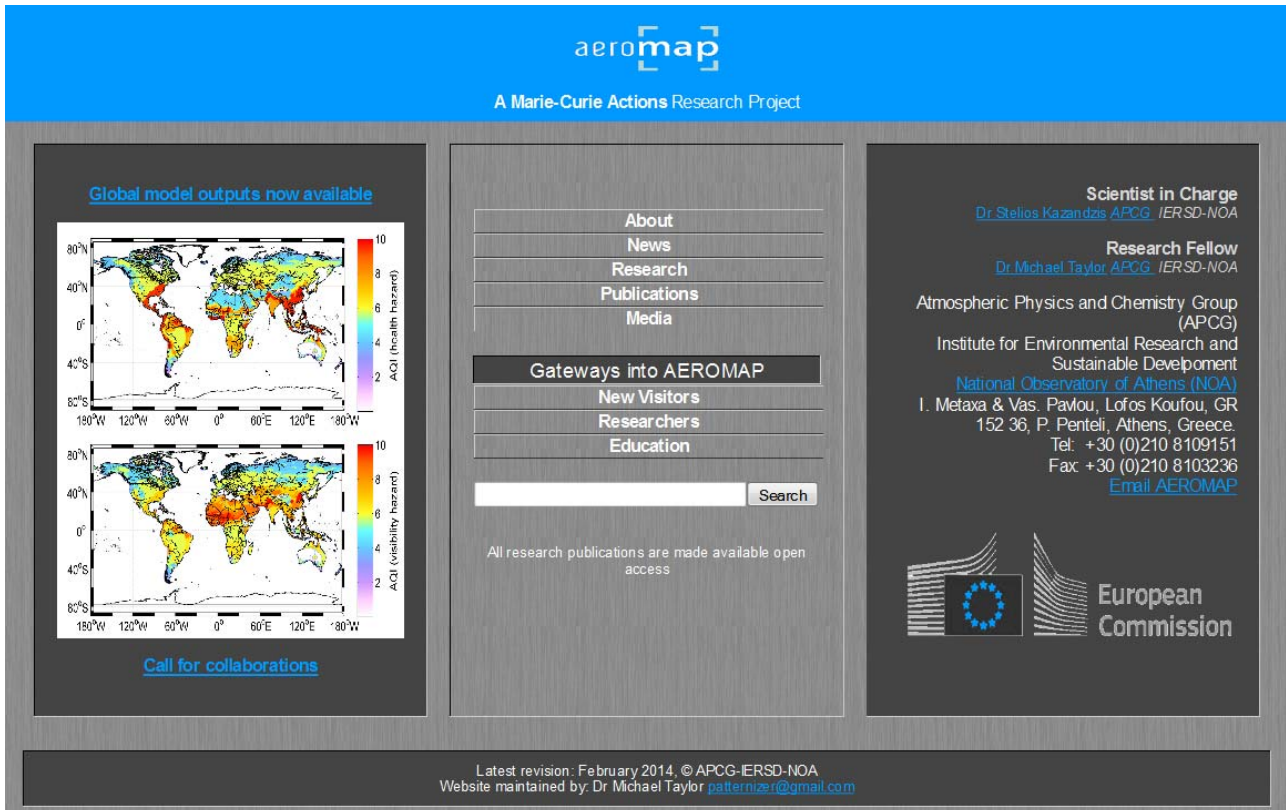


Fig. 36. The home page of the project website.

The website is structured around 5 core pages:

1. The *About* page contains the project abstract and highlights the important role of Marie-Curie Actions in facilitating the mobility of researchers in the ERA, presents the project's objectives and phases and has check-lists showing the progress to completion of the project with regard to expected results and milestones.
2. The *News* page presents a chronological list of events including conference attendances of the fellow, participation in outreach activities, and highlights important landmarks such as the publication of project results in peer-reviewed journals. Readers can be kept up to date of changes by following https://twitter.com/_AEROMAP.
3. The *Research* page lists the lines of investigation being undertaken and the research methods being implemented by AEROMAP.
4. The *Publications* page contains: a) all open-access peer-review publications resulting from the project, b) materials resulting from conference participation including: posters, abstracts and proceedings, c) project reports including i) the mid-term report, ii) the second periodic report and iii) the final report (note that links to the reports will become publicly-available as soon as the research results they contain are published), and d) a link to co-authors.
5. The *Media* page (example screenshot shown below) houses multimedia including an image gallery of graphical abstracts and published images.

aeromap

AEROMAP - Multimedia

AEROMAP - Graphics

AEROMAP

Global mapping of aerosol properties using neural network inversions of ground and satellite based data

Michael Taylor (*Fellow*) patterizer@gmail.com & Stelios Kazadisi (*SIC*)
Institute for Environmental Research & Sustainable Development, National Observatory of Athens, Greece

AEROMAP began on the 1st of March 2012 and is a two year project (FP7-PEOPLE-2011-IEF) designed to produce accurate, daily-updated, global maps of atmospheric aerosols. Aerosols affect human health and the environment [Samet et al., 2000] as they impact strongly on the Earth's energy balance, hydrological cycle and air quality [Reiner et al., 2005]. The uncertainty associated with the estimation of aerosol optical depth (AOD) is considered to be approximately equal in size to the estimated impact of all greenhouse gases combined (Houghton et al., 2001). In order to improve the estimate of the impact of aerosols, they must be correctly characterised globally. Aerosols are characterised by their microphysical properties - the aerosol size distribution (ASD), which since the late 1980s has been measured by the Sun-photometer technique (Z), while accurate measurements of these parameters are currently provided by the 257 international ground-based stations forming the aerosol robotic network (AERONET), the uncertainty is mainly caused by this limited number of stations across the whole Earth's surface, particularly in the Southern Hemisphere. The full Earth's surface is covered by the MODIS satellite depth (AOD) provided by the moderate resolution imaging spectrometer (MODIS) satellite instrument in 3 wavelength bands to globally extrapolate local ground-based estimates of aerosol microphysical properties (ASD) from AERONET stations in the Northern Hemisphere. This will be achieved by constructing and training artificial neural networks (NN) to learn the relationship between AOD inputs and aerosol microphysical properties. In this way, AEROMAP will be able to produce the first global maps of aerosol characteristics on a daily basis.

Acknowledgements
MF would like to thank the Scientist in Charge SK, and all the staff and colleagues at IERSO-NCA for their hospitality, kindness and support.

References

1. Remer, L.A., Kaufman, Y.J., Tanre, D., Mattoo, S., Chu, D.A., et al. (2005): *J. Atmos. Sci.*, 62, 947-958.
2. Ringer, M., J. T. Kiehl, D. J. Griggs, M. Hegerl, P. J. van der Linden, et al. (2003): *Climate Change and the Earth System: The Scientific Basis*. Cambridge University Press.
3. Samet, J. M., S. L. Zeger, F. Dominici, F. Curriero, J. Coursac, D.W. et al. (2000): *Health Effects Institute Research Rep.*, 94, Cambridge, MA.

Poster 1: Euro-Science Open Forum, Dublin

[<<] [<<] [Start] [>>] [>><<]

Top

Fig. 37. The Media page of the project website

In addition, 3 gateways have been developed to provide “click-through” routes for users of differing levels of experience and interest:

- A. The **New Visitors Gateway** links to the *About* and *Media* pages and includes a pictorial guide to the project produced with Prezit to help first-time users quickly understand what the project is about.
- B. The **Researchers' Gateway** links to the *About*, *Research* and *Publications* pages for those with technical understanding of atmospheric aerosols to quickly find up-to-date results and open-source ware produced by the project. In order to provide a vehicle for attracting new researchers in the field to AEROMAP, the gateway also houses a carefully-chosen and comprehensive list of links to data portals for the aerosol community. This “portal of portals” is helping increase the traffic of researchers to the project website. The gateway also houses links to key publications in aerosol science and the empirical techniques used by AEROMAP. Finally, MATLAB code produced by the

fellow to assist researchers to load and parse large data files, is made available at this gateway as open source.

- C. Last but not least, the ***Education Gateway*** presents links to beautiful animated videos of monthly global maps of aerosol optical depth, size and the distribution of fires, chlorophyll, clouds and carbon monoxide. The gateway also links to important reports like those of the International Panel on Climate Change and open-access, online feature articles in magazines like Science and Nature so that readers can get an approachable but accurate overview of the subject. Finally, the gateway links to Open Course Ware online lecture courses on Earth, atmospheric and planetary science and series of graduate lectures on remote sensing, clouds, aerosols and climate.

The *Home* page of the project, in addition to providing contact details, also allows experienced users to go directly to the real-time monitor by clicking on the world map icon. The real-time monitor page displays near real-time global maps of key aerosol microphysical parameters. With regard to maintenance of the website, following each weekly project meeting with the SIC, the fellow will be responsible for making changes to the content and for updating the website.

During the second reporting period, the project website (<http://apcg.space.noa.gr/aeromap>) has been constantly updated with news items, publications and, in particular, the development of the Researchers' Gateway and the Education Gateway:

Researchers' Gateway

Gateways into AEROMAP

- About
- News
- Research
- Publications
- Media

Home

AEROMAP Project

The aim of the AEROMAP Project is to develop an algorithm based on neural networks to produce aerosol inversion data from satellite inputs. By combining the reliability of CIMEL-derived inversion data with the full-Earth viewing capacity of satellite remote sensors, AEROMAP hopes to achieve a global real-time monitor of aerosol microphysical and optical properties.

DATA SOURCES

This endeavor is made possible thanks to the hard work of those colleagues at the hundreds of sites and mission operations worldwide who make quality assured data available to the research community. Below is a list of the main data sources used by AEROMAP.

- **ACTRIS** (Aerosols, Clouds, and Trace gases Research InfraStructure Network)
- **AERONET** (Aerosol Robotic Network) [Holben et al., 1998]
- **AEROSTER** (Online Platform for Satellite Inter-comparison of Aerosols) [Wei et al., 2011]
- **BANDOMS** (Back trajectories, AERONET, MODIS, GOCART, MPLNET/Aerosol Synergy tool) [Giles et al., 2006]
- **CALIPSO** (Cloud-Aerosol Lidar and Infrared Pathfinder Satellite Observations)
- **EARLINET** (European Aerosol Research Lidar Network)
- **FIRMS** (Web Fire Mapper)
- **GIOVANNI** (Interactive Visualization and Analysis) [Berrick et al., 2009]
- **GOCART** (Goddard Global Ozone Chemistry Aerosol Radiation and Transport model) [Chin et al., 2002]
- **MAPSS** (Multi-sensor Aerosol Product Sampling System) [Petrenko et al., 2012]
- **MODIS** (Rapid Response e)
- **MOZART-4GEOSS** (NCAR Atmospheric Composition Remote Sensing and Prediction)
- **MPLNET** (Micro-Pulse Lidar Network)

AEROSOL SCIENCE TOOLS

Researchers in the aerosol science community have developed sites of advanced tools to support global studies of aerosol transport. Below is a list of the main aerosol science tools relevant to AEROMAP:

- COSMO-ART

COSMO-ART [Vogel et al., 2009] is a numerical regional model for aerosols and reactive trace gases developed by the 'Aerosols, Trace Gases and Climate Processes' Group of the Institute for Tropospheric Research, Karlsruhe Institute of Technology (KIT), Germany. The model is online-coupled to the **COSMO** regional numerical weather prediction and climate model [Balajewski et al., 2011] of the German Weather Service (DWD). The online coupling of meteorology and chemistry, allows for the assessment of their interaction (radiative and CCN impact of aerosols). Bibliography on COSMO-ART can be found [here](#). COSMO-ART is available upon request from [Dr. Bernhard Vogel](#) (KIT, Germany).

MATLAB CODE

AEROMAP is almost entirely coded using object-oriented programming scripts of MATLAB R2011b. AEROMAP has developed hundreds of functions and subroutines to perform the necessary calculations. On completion of the project, and having undergone thorough alpha- and beta-testing the AEROMAP code will be made available as open source code protected by a Creative Commons GPU license. The aerosol community may benefit from the following scripts created during Phase A of AEROMAP:

- **AERONET data loader**
- **MODIS data loader**
- **AEROMAP secondary parameter adder**
- **AEROMAP sites ranked by inversion data**
- **GOCART global aerosol mixtures data**

AEROMAP is very grateful to other MATLAB programmers who have made their scripts available open source at the MATLAB File Exchange. The plots produced by AEROMAP owe a large part of their cosmetic appearance to the work of these colleagues. Of the plug-ins used by AEROMAP we wish to acknowledge the following authors:

KEY PUBLICATIONS

AEROMAP builds on a large body of knowledge. Some of the key works that have provided the motivation for this project as well as the theoretical advances that underpin our current understanding of atmospheric aerosols as well as the empirical techniques used to deduce their optical and microphysical characteristics are listed below:

- Hansen, James E., and Larry D. Travis. "Light scattering in planetary atmospheres." *Space Science Reviews* 16 (1974): 527-510.
- Dubovik, Oleg, and Michael D. King. "A flexible inversion algorithm for retrieval of aerosol optical properties from Sun and sky radiance measurements." *Journal of Geophysical Research: Atmospheres* (1984-2012) 105, D16 (2000): 20673-20696.
- Hornik, Kurt, Maxwell Stinchcombe, and Halbert White. "Multilayer feedforward networks are universal approximators." *Neural networks* 2, 5 (1989): 369-366.
- Moshchenko, Michael I., et al. "Accurate monitoring of terrestrial aerosols and total solar irradiance: introducing the Glory Mission." *Bulletin of the American Meteorological Society* 88, 5 (2007): 677-691.

Top

Figure 38: The Researchers' Gateway at the project website

The Researchers' Gateway provides, in one place, links to online data centres used by the remote sensing and aerosol science community to facilitate “click-throughs” by users who are using this page as of the AEROMAP website as a portal. The page also links to specialized aerosol science tools and makes available MATLAB scripted utilities produced by AEROMAP to help researchers load data for their own studies. On this page, datasets to be produced by AEROMAP and referred to in future publications, will be permanently housed so as to provide persistence of the project's end-products.

The screenshot shows the 'Educational Resource Gateway' homepage. At the top right is the 'aeromap' logo. The main header is 'Educational Resource Gateway'. On the left is a vertical sidebar with links: 'About', 'News', 'Research', 'Publications', 'Media', 'Gateways into AEROMAP', 'New Visitors', 'Researchers', 'Education', and 'Home'. Below this is a large puzzle piece icon. The main content area has a grey background. It features a section titled 'VIDEOS' with a brief description about the AEROMAP Project's aim to develop a satellite-based real-time monitor of global aerosols and their microphysical properties, followed by a list of links to various aerosol-related videos. Below this is a 'WEB RESOURCES' section containing a long list of scientific articles and reports. At the bottom of the content area is a 'LECTURE COURSES' section with a list of links to Open Course Ware lectures. A 'Top' button is located at the bottom right of the content area.

Figure 38: The Educational Gateway at the project website

The Education Gateway is dedicated to outreach activities of the project and is designed to help inform interested readers about aerosol science and the global impact of aerosols with videos and other online electronic resources. On this page, open-access popular science articles about the impact of aerosols on climate are also linked to and, for students thinking of pursuing a career in environmental research, hyperlinks to relevant Open Course Ware lecture notes have been selected and provided. The content and volume of traffic associated with the project website are helping to raise awareness of the project, the fellow, the scientist in charge, the host institute, co-authors, and the impact on society of scientific research on the global aerosol system being funded and undertaken in the ERA.

2.3.7 Training activities

One of the main training objectives of the project was to aid the transition of the fellow as an applied mathematics to principal investigator level in the field of environmental modelling so that he could have acquired the competences to ensure tenure in this area. The fellow has designed, managed and performed the research competently and productively. The results have led to satisfaction of the project objectives for these phases and have produced several important and high-impact bi-products. The fellow has been

exposed to a broad array of contemporary methods, techniques and analyses in the field of aerosol science while at the host institute including: i) adaptation to the technical basics of ground-based aerosol instrumentation, measurement, retrieval and databases, ii) adaptation to satellite remote sensing retrieval techniques and databases, and iii) the development of algorithms for advanced analysis. This experience has substantially increased the fellow's knowledge of aerosol science, remote sensing, atmospheric physics and the impact of aerosols on climate. New collaborations in the field of environmental modelling have been established and have led to co-authorship on two important published articles led by international teams in the Journals of Atmospheric Measurement Techniques and Atmospheric Chemistry and Physics. Through presentation of his results in 3 first-author publications and 2 conference papers, the fellow has helped to introduce neural networks models and other applied mathematics techniques to a community with limited experience of these approaches. Furthermore, the fellow has given talks in bi-monthly meetings of the APC Group at IERSD-NOA. In particular, he has given two Power-point presentations providing report-backs on the progression of the project, the new methods developed and the main results of the work performed in each Phase. These report-backs marked important points in the progression of the project and have helped ensure its smooth running.

The high international standing of members of the APC Group has provided the fellow with the opportunity to attain a high technical level of scientific communication skills via co-authorship and lead-authorship of several peer-reviewed research articles. These opportunities arose as a direct consequence of the great deal of in-house expertise of the APC Group members who are internationally recognized through their editorships on scientific journals, their invited talks at international conferences, invited review papers in top journals, high citation rates, and through their coordination of EU-funded research projects. The fellow, by working at the host institute, has been in contact with broad scientific expertise in the fields of aerosol science, climate change, satellite remote sensing and ground-based instrumentation, measurement and data analysis and atmospheric chemistry. This has enabled collaboration and interaction with other principal investigators in the field at both the national and international level (see next section).

2.3.8 Co-operation with other projects/programmes

The SIC has included the methods introduced in the project in grant funding proposals with a view to hopefully creating a post-project job opening for the fellow at the host institute. The host institute's success in obtaining state funding for a large national project meant that the fellow was able to secure a research contract at the host institute following on directly the completion of AEROMAP in March 2014. In addition, the AEROMAP project was included in the research portfolio of the host institute during a recent national assessment of research centres.

Techniques developed during the course of the project meant that the fellow could contribute to 2 important articles as co-author. In the first article, published in the *Journal of Atmospheric Chemistry and Physics*, which presented a methodology for optimising dust retrievals with improvements to the CALIPSO LIDAR algorithm, the fellow played a key role in the writing/editing of the manuscript as co-author in a large international consortium:

Amiridis, V., Wandinger, U., Marinou, E., Giannakaki, E., Tsekeli, A., Basart, S., Kazadzis, S., Gkikas, A.,
Taylor, M., Baldasano, J., & Ansmann, A. (2013). Optimizing Saharan dust CALIPSO retrievals. *Atmospheric Chemistry and Physics* 13, 12089-12106.

In the second article, published in the *Journal of Atmospheric Measurement Techniques Discussions*, which compared aerosol microphysical retrievals from the World Meteorological Organisation's precision filter radiometer with those of AERONET's inversion algorithm, the fellow acquired and processed data to make it synchronous and produced contour plots and time series of key microphysical parameters. The article was the result of international collaboration with colleagues from the Physics Instrumentation Centre in Moscow and the World Radiation Centre at Davos among others:

Kazadzis, S., Veselovskii, I., Amiridis, V., Gröbner, J., Suvorina, A., Nyeki, S., Gerasopoulos, E., Kouremeti, N., **Taylor, M.**, Tsekeri, A., Wehrli, C. (2014). Aerosol microphysical retrievals from Precision Filter Radiometer direct solar radiation measurements and comparison with AERONET. *Atmospheric Measurement Techniques Discussions* 7, 99-130, 2014.

It is important also to mention that two Greek experts in remote sensing: Dr Alexandra Tsekeri and Dr Antonios Gkikas have made a significant contribution to some of the project's deliverables by making high quality MODIS and OMI satellite data available to the fellow (Dr. Gkikas) and by providing information on the limitations of various measurement approaches and their inherent uncertainties (Dr. Tsekeri).

Finally, collaboration with the Director of the APC Group Dr. Evangelos Gerasopoulos who is expert in atmospheric chemistry led to the development of an important new technique for improving the fitting and interpretation of AERONET-retrieved aerosol size distributions. This collaboration created new synergies between the fields of remote sensing and atmospheric chemistry leading to 4 research reports with the fellow as first author:

Taylor, M., Kazadzis, S., Gerosopoulos, E. (2013). Multi-modal analysis of aerosol robotic network size distributions for remote sensing applications: dominant aerosol type cases. *Atmospheric Measurement Techniques Discussions* 6, 10571–10615, 2013.

Taylor, M., Kazadzis, S., Gerosopoulos, E. (2014). Multi-modal analysis of aerosol robotic network size distributions for remote sensing applications II: temporal evolution of high load events. *Atmospheric Chemistry and Physics Discussions* (manuscript in the process of submission).

Taylor, M., Kazadzis, S., Gerosopoulos, E. (2014). Multi-modal fitting of AERONET size distributions during atypical aerosol conditions. Proc. 12th Int. Conf. on Meteorology, Climatology and Atmos. Phys. (COMECA), 28-31/05/2014, Heraklion, Crete, Greece. (under review).

3 Deliverables and milestones tables

3.1 Deliverables

The deliverables due in this reporting period include:

D5: Partitioning of the globe into distinct aerosol types/mixtures using cluster analysis

D6: Rendering of global ANN-derived AMP maps with aerosol typing

D7: Pilot studies of aerosol temporal variation (tracking) for a number of climatologically and/or socio-economically important cases

D8: Production of accurate, daily-updated, global maps of AMP on a global grid of resolution 1 degree CMG

D9: A global real-time monitor of aerosols and alerting service for the assessment of climatological risks and the issuing of early-warnings

D10: Creation of a project website/portal and the organization by the fellow of two public open days.

3.2 Bi-products of the research performed

In addition, to the main core novelty of AEROMAP – the development of neural networks to invert satellite data and retrieve aerosol optical and microphysical properties in pixels of the global grid, the fellow has developed and contributed to other important techniques during the course of completing Phases C and D:

1. A method for performing uncertainty analysis based on measuring averages at different timescales was developed in the course of Task B3. This technique was central to understanding the performance of the neural networks in terms of daily trends in retrieved aerosol parameters, and was given prominence in the core paper describing the NN methodology used by AEROMAP in the context of dust aerosol in Northern Africa (see Section 1.2.1 and Section 2.1 for details).
2. A method for improving the retrieval of dust aerosol properties over the Sahara via LIDAR measurement with CALIPSO was published in the Journal of Atmospheric Chemistry and Physics (see Section 1.2.1 and Section 2.1 for details).
3. A comparison of AERONET secondary microphysical properties derived from the size distribution with those produced by inversion of Precision Filter Radiometer measurements for published in the Journal of Atmospheric Measurement Techniques Discussions (see Section 1.2.1 and Section 2.1 for details).
4. An algorithm for identifying and characterising multiple-modes in the size distribution has been developed and tested with success on pilot studies such as a severe desert dust storm, the Beijing urban brown cloud, the outbreak of fires in the Africa Savannah and the eruption of volcanic ash from Iceland. The algorithm lifts the constraint of current research to studies of only two aerosol modes (fine particles and coarse particles) and allows researchers to monitor the temporal changes in the size distribution that result from the influx of aerosol during extreme conditions. An article describing the methodology has been published in the Journal of Atmospheric Measurement Techniques (see Section 1.2.1) for dominant aerosol

types (dust, biomass burning, urban sulphate and marine aerosol) and a second article on fitting temporally-evolving size distributions during high load aerosol events is in the process of being submitted (see Section 1.2.1). A conference paper has also been submitted for publication in the proceedings of the 12th International Conference on Meteorology, Climatology and Atmospheric Physics (see Section 1.2.1 and Section 2.1 for details).

5. A global classification of aerosols via cluster analysis of GOCART chemical data has been achieved allowing identification of the number of NNs required to model the entire Earth surface and to which pixels they should apply (see Section 1.2.1 and Section 2.1 for details).

Publications describing these new techniques are direct by-products of the work performed in pursuit of the project's main objectives and are additions to the list of deliverables to be reported on in the final report.